



SUBCARRIER ALLOCATION IN OFDMA SYSTEMS WITH TIME VARYING  
CHANNEL AND PACKET ARRIVALS

A THESIS SUBMITTED TO  
THE GRADUATE SCHOOL OF NATURAL AND APPLIED SCIENCES  
OF  
MIDDLE EAST TECHNICAL UNIVERSITY

BY

ENGİN TOKTAŞ

IN PARTIAL FULFILLMENT OF THE REQUIREMENTS  
FOR  
THE DEGREE OF MASTER OF SCIENCE  
IN  
ELECTRICAL AND ELECTRONICS ENGINEERING

SEPTEMBER 2008

Approval of the thesis:

**SUBCARRIER ALLOCATION IN OFDMA SYSTEMS WITH TIME VARYING  
CHANNEL AND PACKET ARRIVALS**

submitted by **ENGİN TOKTAŞ** in partial fulfillment of the requirements for the degree of  
**Master of Science in Electrical and Electronics Engineering Department, Middle East  
Technical University** by,

Prof. Dr. Canan Özgen  
Dean, Graduate School of **Natural and Applied Sciences** \_\_\_\_\_

Prof. Dr. İsmet Erkmén  
Head of Department, **Electrical and Electronics Engineering** \_\_\_\_\_

Assist. Prof. Dr. Ali Özgür Yılmaz  
Supervisor, **Electrical and Electronics Engineering Department,  
METU** \_\_\_\_\_

Assoc. Prof. Dr. Elif Uysal Bıyıköđlü  
Co-supervisor, **Electrical and Electronics Engineering Department,  
METU** \_\_\_\_\_

**Examining Committee Members:**

Prof. Dr. Yalçın Tanık  
Electrical and Electronics Engineering Department, METU \_\_\_\_\_

Assist. Prof. Dr. Ali Özgür Yılmaz  
Electrical and Electronics Engineering Department, METU \_\_\_\_\_

Assoc. Prof. Dr. Elif Uysal Bıyıköđlü  
Electrical and Electronics Engineering Department, METU \_\_\_\_\_

Prof. Dr. Mete Severcan  
Electrical and Electronics Engineering Department, METU \_\_\_\_\_

Dr. Ülkü Doyuran  
ASELSAN A.Ş. \_\_\_\_\_

**Date:** \_\_\_\_\_

**I hereby declare that all information in this document has been obtained and presented in accordance with academic rules and ethical conduct. I also declare that, as required by these rules and conduct, I have fully cited and referenced all material and results that are not original to this work.**

Name, Last Name: ENGİN TOKTAŞ

Signature :

# ABSTRACT

## SUBCARRIER ALLOCATION IN OFDMA SYSTEMS WITH TIME VARYING CHANNEL AND PACKET ARRIVALS

Toktaş, Engin

M.S., Department of Electrical and Electronics Engineering

Supervisor : Assist. Prof. Dr. Ali Özgür Yılmaz

Co-Supervisor : Assoc. Prof. Dr. Elif Uysal Bıyıkoğlu

September 2008, 75 pages

This study considers the average system throughput and the average delay performances of subcarrier allocation algorithms in OFDMA systems. The effects of varying the number of users, the number of subcarriers, and the statistical characteristics of incoming packets are investigated on the throughput and delay performances of the algorithms. Moreover, a new subcarrier allocation algorithm with low-order computational complexity, which performs very well almost all cases, is proposed. With the aid of the simulations, the significance of channel v.s. queue state information varying with the statistical characteristic of incoming packets is examined and reached some results which can be very valuable for channel estimation and feedback systems. Finally, the stability issue is considered in OFDMA systems and a new heuristic simulation-based method for obtaining the stability region of an OFDMA subcarrier allocation algorithm is proposed.

Keywords: OFDMA, subcarrier allocation, throughput, delay, stability

## ÖZ

### OFDMA SİSTEMLERDE ZAMANLA DEĞİŞEN KANAL VE GELEN PAKET MİKTARLARINA GÖRE ALT-TAŞIYICILARIN PAYLAŞTIRILMASI

Toktaş, Engin

Yüksek Lisans, Elektrik - Elektronik Mühendisliği Bölümü

Tez Yöneticisi : Yard. Doç. Dr. Ali Özgür Yılmaz

Ortak Tez Yöneticisi : Doç. Dr. Elif Uysal Bıyıkoğlu

Eylül 2008, 75 sayfa

Bu tez çalışmasında, Dikgen Sıklık Bölümlü Çoklu Erişim (OFDMA) sistemlerindeki alt-taşıyıcıların paylaşılması yöntemlerinin ortalama sistem paket çıktı ve gecikme performansları üzerine çalışılmıştır. Sistemdeki kullanıcı sayısının, alt-taşıyıcı sayısının ve sisteme gelen paket miktarlarının istatistiksel karakteristiğinin değişimi sonucunda alt-taşıyıcı paylaşma yöntemlerinin paket çıktı miktarı ve gecikme performanslarındaki değişimler incelenmiştir. Ayrıca, performansı, incelenen hemen hemen her durumda çok iyi çıkan ve hesap karmaşıklığı düşük olan yeni bir alt-taşıyıcı yöntemi önerilmiştir. Yapılan benzeşimler ışığında, sistemin kanala karşı kuyruk bilgisi değerinin sisteme gelen paket miktarlarının istatistiksel karakteristiğine göre değişimi incelenmiş ve kanal kestirim ve geribesleme sistemleri için değerli olabilecek bazı sonuçlar elde edilmiştir. Son olarak, OFDMA sistemlerde “kararlılık” konusu üzerinde çalışılmış ve alt-taşıyıcıların paylaşılması yöntemlerinin her birinin kararlılık bölgesini bulmaya yarayan, benzeşim tabanlı, sezgisel bir yöntem önerilmiştir.

Anahtar Kelimeler: OFDMA, alttaşıyıcı paylaşımı, üretilen iş, gecikme, kararlılık

*To my Father, my Mother,  
my Sister, my Brother Özgür, Yağmur  
and  
Selma*

## **ACKNOWLEDGMENTS**

I would like to express my gratitude to my supervisors Assist. Prof. Dr. Ali Özgür Yılmaz and Assoc. Prof. Dr. Elif Uysal Bıyıkođlu for their valuable guidance and suggestions. Without their support, this thesis would not have been completed.

I am particularly grateful to my dear family for providing me the best possible education and for keeping their faith on me throughout my life. I would especially like to thank to Selma Arslantaş for her endless support and love.

I would like to give my special appreciation to TÜBİTAK for the scholarship that they supplied for two years of my study. Also, I would like to thank to ASELSAN Inc. for allowing me to spend time on this thesis.

The last but not least, I am indebted to my friends and colleagues for their constant support and encouragement that kept me going during the hard times.

# TABLE OF CONTENTS

ABSTRACT . . . . .	iv
ÖZ . . . . .	v
DEDICATON . . . . .	vi
ACKNOWLEDGMENTS . . . . .	vii
TABLE OF CONTENTS . . . . .	viii
LIST OF TABLES . . . . .	xi
LIST OF FIGURES . . . . .	xii
CHAPTERS	
1 INTRODUCTION . . . . .	1
1.1 SCOPE AND OBJECTIVE . . . . .	1
1.2 OUTLINE OF THE THESIS . . . . .	3
2 OVERVIEW OF OFDM AND OFDMA . . . . .	4
2.1 ORTHOGONAL FREQUENCY DIVISION MULTIPLEXING (OFDM) . . . . .	4
2.1.1 HISTORY OF OFDM . . . . .	4
2.1.2 STRUCTURE OF OFDM . . . . .	6
2.1.3 APPLICATIONS OF OFDM . . . . .	9
2.1.3.1 DIGITAL AUDIO BROADCASTING (DAB) . . . . .	9
2.1.3.2 TERRESTRIAL DIGITAL VIDEO BROADCASTING (DVB-T) . . . . .	10
2.1.3.3 IEEE 802.11 WIRELESS LAN STANDARD . . . . .	10
2.1.4 ADVANTAGES AND DISADVANTAGES OF OFDM . . . . .	11
2.2 ORTHOGONAL FREQUENCY DIVISION MULTIPLE ACCESS (OFDMA) . . . . .	12
2.2.1 IEEE 802.16e WIRELESS MAN STANDARD . . . . .	13

3	SYSTEM MODEL AND PROBLEM FORMULATION . . . . .	14
3.1	SYSTEM MODEL . . . . .	14
3.1.1	INCOMING PACKET TRAFFIC MODEL . . . . .	15
3.1.2	CHANNEL MODEL . . . . .	18
3.1.3	CONSTRUCTION CRITERIA OF CHANNEL CONN- ECTIVITY MATRIX . . . . .	22
3.1.4	CONSTRUCTION CRITERIA OF ALLOCATION MA- TRIX . . . . .	25
3.2	PROBLEM FORMULATION . . . . .	27
3.2.1	SYSTEM AVERAGE THROUGHPUT MAXIMIZATION PROBLEM . . . . .	27
3.2.2	SYSTEM AVERAGE DELAY MINIMIZATION PROB- LEM . . . . .	28
4	SUBCARRIER ALLOCATION ALGORITHMS . . . . .	29
4.1	INTRODUCTION TO SUBCARRIER ALLOCATION . . . . .	29
4.2	BIG-O NOTATION . . . . .	29
4.3	MAXIMUM INSTANTANEOUS THROUGHPUT ALGORITHM (MIT) . . . . .	31
4.4	LOAD EQUALIZING ALGORITHM (LE) . . . . .	32
4.5	MAXIMUM WEIGHT MATCHING ALGORITHM (MWM) . . . . .	33
4.6	RECURSIVE MAXIMUM WEIGHT MATCHING (r-MWM) . . . . .	35
4.7	UPDATED MAXIMUM WEIGHT MATCHING (u-MWM) . . . . .	37
5	SIMULATIONS AND RESULTS . . . . .	39
5.1	SIMULATIONS AND SOME RELATED PARAMETERS . . . . .	39
5.1.1	SIMULATION ENVIRONMENT . . . . .	39
5.1.2	SYSTEM AVERAGE THROUGHPUT AND SYSTEM AV- ERAGE DELAY . . . . .	40
5.1.3	CALCULATION METHOD FOR “LOAD” PARAMETER . . . . .	41
5.1.4	CALCULATION METHOD FOR THE PARAMETER “BAL- ANCE RATIO” . . . . .	44
5.2	SIMULATION RESULTS . . . . .	45
5.2.1	THE EFFECT OF THE NUMBER OF USERS (N) . . . . .	45
5.2.1.1	SIMULATION #1 (N=2) . . . . .	46

5.2.1.2	SIMULATION #2 (N=4) . . . . .	47
5.2.1.3	SIMULATION #3 (N=8) . . . . .	48
5.2.1.4	SIMULATION RESULTS OF SIM. #1, #2 AND #3 . . . . .	49
5.2.2	THE EFFECT OF THE NUMBER OF SUBCARRIERS (K) . . . . .	50
5.2.2.1	SIMULATION #4 (K=8) . . . . .	51
5.2.2.2	SIMULATION #5 (K=16) . . . . .	52
5.2.2.3	SIMULATION #6 (K=32) . . . . .	53
5.2.2.4	SIMULATION RESULTS OF SIM. #4, #5 AND #6 . . . . .	54
5.2.3	THE EFFECT OF THE BALANCE RATIO (r) . . . . .	54
5.2.3.1	SIMULATION #7 (r={0.5, 0.5}) . . . . .	55
5.2.3.2	SIMULATION #8 (r={0.7, 0.3}) . . . . .	56
5.2.3.3	SIMULATION #9 (r={0.9, 0.1}) . . . . .	57
5.2.3.4	SIMULATION RESULTS OF SIM. #7, #8 AND #9 . . . . .	58
5.2.3.5	THE EFFECT OF ELEPHANT-MOUSE POPULATION . . . . .	59
5.2.4	OBTAINING THE STABILITY REGION WITH A SIMULATION-BASED TECHNIQUE . . . . .	62
5.2.4.1	SIMULATION BASED STABILITY CHECKING METHOD . . . . .	64
5.2.4.2	COMPARISONS OF THE STABILITY REGIONS OF THE ALGORITHMS . . . . .	66
6	CONCLUSION AND FUTURE WORK . . . . .	68
	REFERENCES . . . . .	71
	APPENDICES	
A	LITTLE'S THEOREM . . . . .	74

## LIST OF TABLES

### TABLES

Table 2.1	DAB OFDM parameters . . . . .	10
Table 2.2	DVB-T parameters . . . . .	10
Table 2.3	IEEE 802.11a parameters . . . . .	11
Table 2.4	IEEE 802.16e parameters . . . . .	13
Table 3.1	Probability of the occurrence of each channel connectivity value . . . . .	25
Table 5.1	Average output capacity (pkt/slot) per subcarrier w.r.t number of users . . . . .	43
Table 5.2	Parameters for Simulation # 1 . . . . .	46
Table 5.3	Parameters for Simulation # 2 . . . . .	47
Table 5.4	Parameters for Simulation # 3 . . . . .	48
Table 5.5	Parameters for Simulation # 4 . . . . .	51
Table 5.6	Parameters for Simulation # 5 . . . . .	52
Table 5.7	Parameters for Simulation # 6 . . . . .	53
Table 5.8	Parameters for Simulation # 7 . . . . .	55
Table 5.9	Parameters for Simulation # 8 . . . . .	56
Table 5.10	Parameters for Simulation # 9 . . . . .	57
Table 5.11	Parameters for Simulation # 10 . . . . .	60
Table 5.12	Parameters for Simulation # 11 . . . . .	61

## LIST OF FIGURES

### FIGURES

Figure 2.1	Representation of frequency selective fading . . . . .	5
Figure 2.2	Spectral efficiency of OFDM . . . . .	5
Figure 2.3	General structure of OFDM system . . . . .	7
Figure 2.4	Comparison of OFDM and OFDMA Systems . . . . .	12
Figure 3.1	Block Diagram of the System . . . . .	15
Figure 3.2	Packet Arrivals For Each User . . . . .	16
Figure 3.3	State Transition of the Poisson Process . . . . .	17
Figure 3.4	Poisson Random Traffic Generator . . . . .	18
Figure 3.5	Multipath Propagation . . . . .	19
Figure 3.6	Multipath Block Diagram . . . . .	19
Figure 3.7	Rayleigh Distribution Graphic . . . . .	22
Figure 3.8	Typical Adaptive Modulation Scheme . . . . .	23
Figure 3.9	Adaptive Modulation Mapper Block Diagram . . . . .	24
Figure 3.10	Adaptive Modulation Limits on Rayleigh Graph . . . . .	25
Figure 3.11	Allocation Matrix Generation Block Diagram . . . . .	26
Figure 4.1	Maximum Weight Matching . . . . .	35
Figure 5.1	An example of the graphical user interface . . . . .	40
Figure 5.2	Output capacity (per subcarrier) characteristic w.r.t. $N$ . . . . .	43
Figure 5.3	Simulation # 1 ( $N=2$ ) . . . . .	46
Figure 5.4	Simulation # 2 ( $N=4$ ) . . . . .	47
Figure 5.5	Simulation # 3 ( $N=8$ ) . . . . .	48

Figure 5.6 Simulation # 4 ( $K=8$ ) . . . . .	51
Figure 5.7 Simulation # 5 ( $K=16$ ) . . . . .	52
Figure 5.8 Simulation # 6 ( $K=32$ ) . . . . .	53
Figure 5.9 Simulation # 7 ( $r=\{0.5, 0.5\}$ ) . . . . .	55
Figure 5.10 Simulation # 8 ( $r=\{0.7, 0.3\}$ ) . . . . .	56
Figure 5.11 Simulation # 9 ( $r=\{0.9, 0.1\}$ ) . . . . .	57
Figure 5.12 Simulation # 10 ( $r=\{0.75, 0.0357, \dots, 0.0357\}$ ) . . . . .	60
Figure 5.13 Simulation # 11 ( $r=\{0.02, 0.14, \dots, 0.14\}$ ) . . . . .	61
Figure 5.14 The effect of load and balance ratio on throughput region . . . . .	63
Figure 5.15 Batching the slot time . . . . .	64
Figure 5.16 Examples of the instability . . . . .	65
Figure 5.17 Simulation # 12 ( $N=2, K=32$ ) . . . . .	66
Figure A.1 Little's Theorem Representation . . . . .	75

# CHAPTER 1

## INTRODUCTION

### 1.1 SCOPE AND OBJECTIVE

In recent years, together with the developing related technology, wireless communication networks have enjoyed a rapid surge of interest and deployment. Today, the most popular wireless networks are generally in the group of Personal Area Network (PAN) (e.g. bluetooth, Zigbee) or Local Area Network (LAN) (e.g. IEEE 802.11). Similarly, increasing the number of customers and increasing the demand on more mobile communication systems make Metropol Area Network (MAN) technologies become popular. Orthogonal Frequency Division Multiple Access (OFDMA) is one of the most important MAN technologies and is part of the IEEE 802.16a and IEEE 802.16e standards.

In addition to possessing the advantages of the Orthogonal Frequency Division Multiplexing (OFDM) such as good spectral efficiency and immunity to multipath fading, OFDMA allows the allocation of subcarriers to various users for simultaneous transmission. In other words, OFDMA system divides the total available bandwidth into multiple orthogonal narrow subcarriers to be shared by users at the same timeslot.

The motivation of our study is based on an OFDMA system with one base station,  $N$  users and  $K$  subcarriers. In such a system, data packets arrive stochastically to each user and are stored in queues prior to transmission. However, because of the limited number of subcarriers, the system may not be able to make a simultaneous transmission of all queued packets. So, the system should make a choice of assignment of subcarriers to users. This gives rise to a scheduling problem involving the allocation of the orthogonal channels to different data streams.

There have been some studies related with the subcarrier allocation problem in the literature. [1], [2], [3], [4] provide solutions to a multi-user waterfilling problem achieving Shannon capacity under power constraint at each decision epoch. All these solutions try to maximize the “instantaneous” throughput of the system. When each user is assumed to have an infinite amount of data in the buffer, waterfilling becomes throughput optimal [9]. However when considering stochastic packet arrivals with finite length, [8] shows that waterfilling is not throughput optimal. So, other group of studies related with subcarrier allocation such as [5],[8],[6] focus on the long term throughput maximization rather than the instantaneous throughput maximization. There exist also some other studies which are more interested in another important issue along with throughput about the system performance: the “delay” performance. However, these studies investigate very specific scenarios and their proposals about the system throughput and delay issues can not be directly generalized to other scenarios. For example, [7] proposes a subcarrier allocation method when the base station has only one subcarrier. Moreover, [6] studies on a system which has an ON/OFF channel model, that is, the connectivity value of an ON/OFF channel can be either 1 or 0. So adaptive modulation schemes with multiple choices for spectral efficiency can not be applied to this channel model. To sum up, to the best of our knowledge, subcarrier allocation algorithms are insufficiently addressed in the literature with respect to different aspects such as throughput, delay and complexity.

Throughout our study, we are interested in subcarrier allocation algorithms in terms of both system average throughput and average delay performances. During our investigations, we take into account many parameters such as the number of users, the number of subcarriers, packet traffic load, incoming traffic ratios among users, etc. Moreover, we propose a subcarrier allocation algorithm which performs very well in most of the cases in addition to low computational complexity. At the end of the algorithm investigations, we obtain some observations about the significance of the channel state information vs. the queue state information on system performances varying with some specific parameters. This is of practical interest when one considers the overhead associated with channel estimation and feedback.

Another major part of this study is obtaining the stability regions of the subcarrier allocation algorithms via a simulation-based method rather than an analysis method. In this study, we propose a method, which is very easy to be applied to OFDMA systems, for checking the stability of a queueing network. We apply this method to subcarrier allocation algorithms of

our interest and obtain their stability boundaries.

## **1.2 OUTLINE OF THE THESIS**

This thesis consists of six chapters.

In Chapter 1, the scope and the objective of the thesis are presented.

In Chapter 2, the general structure of OFDM and OFDMA systems is explained.

In Chapter 3, the system model used in our simulations is described.

In Chapter 4, subcarrier allocation algorithms and their decision mechanisms are explained.

In Chapter 5, the simulation method for investigating the system average throughput and average delay is discussed first and then the simulation results are presented. Also, the stability determination method is laid out.

In Chapter 6, conclusions on this study and future directions are outlined.

## CHAPTER 2

### OVERVIEW OF OFDM AND OFDMA

#### 2.1 ORTHOGONAL FREQUENCY DIVISION MULTIPLEXING (OFDM)

##### 2.1.1 HISTORY OF OFDM

Orthogonal Frequency Division Multiplexing (OFDM), is a special case of multicarrier transmission, where a single data stream is transmitted over a number of lower rate subcarriers. OFDM can be seen as either a modulation technique or a multiplexing technique. One of the main reasons to use OFDM is to increase robustness against frequency selective fading or narrowband interference. In a single carrier system, a single fade or interferer can cause the entire link to fail, but in a multicarrier system, only a small percentage of the subcarriers will be effected. Error correction coding can then be used to correct for the few erroneous subcarriers. In Figure 2.1, in the first sub-figure the signal and the channel frequency response are well matched. However, in the second sub-figure there exists a fading channel and this can cause data loss. In the third sub-figure, the same fading causes only small part of the data losses with OFDM.

The concept of using parallel data transmission and frequency division multiplexing (FDM) was developed in the mid-1960's. A U.S. patent was filed and issued in January 1970 ([10]).

In a classical parallel data system, the total signal frequency band is divided into  $K$  nonoverlapping frequency subchannels. Each subchannel is modulated with a separate symbol, and then the  $K$  subchannels are frequency multiplexed. At first glance, it seems good to avoid spectral overlap of channels to eliminate interchannel interference. However, this leads to inefficient use of the available spectrum. To cope with this inefficiency, the ideas proposed

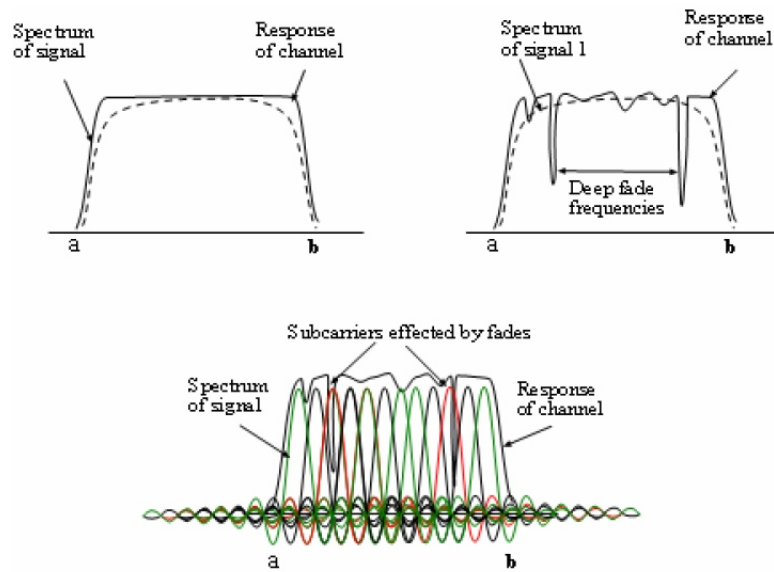


Figure 2.1: Representation of frequency selective fading

in mid-1960's were to use parallel data and FDM with overlapping subchannels, carrying a signalling rate  $b$  and spaced carefully apart in frequency in order to avoid the use of high complexity equalization and combat impulsive noise and multipath distortion, as well as to fully utilize the available bandwidth.

Figure 2.2 illustrates the difference between conventional nonoverlapping multicarrier technique and the overlapping multicarrier modulation technique. By using the overlapping multicarrier modulation technique, we save almost 50% of bandwidth. However, this technique requires orthogonality between different subcarriers in order to reduce cross talk between subcarriers.

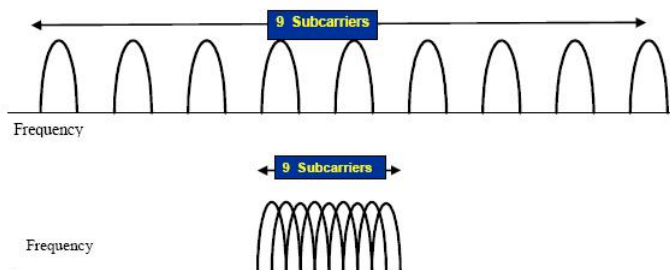


Figure 2.2: Spectral efficiency of OFDM

It is possible to arrange the carriers in an OFDM signal so that the sidebands of individual carriers overlap and the signals are still received without adjacent carrier interference. To do this, the carriers must be mathematically orthogonal. The receiver acts as a bank of demodulators, translating each carrier down to baseband, with the resulting signal integrated over a symbol period to recover raw data. Section 2.1.2 gives more details about the main principles of OFDM.

In 1971, Weinstein and Ebert [11] applied the discrete Fourier transform (DFT) to parallel data transmission systems as part of the modulation and demodulation process. Using the DFT-based multicarrier technique, FDM is achieved not by bandpass filtering but by baseband processing. Moreover, for the banks of subcarrier oscillators and coherent demodulators required by FDM, digital implementations could be built around special purpose hardware performing the fast Fourier transform (FFT), which is an efficient implementation of DFT. Recent advances in very large scale integration (VLSI) technology make high speed, large size FFT chips commercially affordable. Using this method, both transmitter and receiver are implemented using efficient FFT techniques that reduce the number of operations.

In the 1990's, OFDM was exploited for wideband data communications over mobile radio FM channels, high bit-rate digital subscriber lines (HDSL, 1.6 Mbps), asymmetric digital subscriber lines (ADSL, up to 6 Mbps), very high speed digital subscriber lines (VDSL, 100 Mbps), digital audio broadcasting (DAB) and high definition television (HDTV) terrestrial broadcasting.

### 2.1.2 STRUCTURE OF OFDM

Multicarrier modulation (MCM) is a communication approach where the available channel bandwidth is subdivided into a number of parallel subchannels so that data is transmitted over these subchannels. A multicarrier modulated signal can be represented as follows,

$$s(t) = \sum_j g(t - jT) \sum_{i=1}^K [a_{ij} \cos(2\pi f_i t) + b_{ij} \sin(2\pi f_i t)] \quad (2.1)$$

where  $K$  is the number of subcarriers and also the number of carriers  $f_i$  ( $i=1,2,\dots,K$ ) are the carrier frequencies,  $a_{ij}$  and  $b_{ij}$  are modulating symbols of an  $M_i$ -ary symbol set,  $g(t)$  is the

modulating pulse shape and  $T$  is the symbol duration.

As explained in the previous section, OFDM is a special type of MCM. Generally in MCM, the subcarrier spacing is selected sufficiently high such that the spectra of subcarriers do not overlap. However, in OFDM the subcarrier spacing is kept at the minimum level, which preserves the orthogonality between subcarriers in time, even though the individual subcarrier spectra may overlap. The general structure of OFDM transmitter and receiver system is given in Figure 2.3.

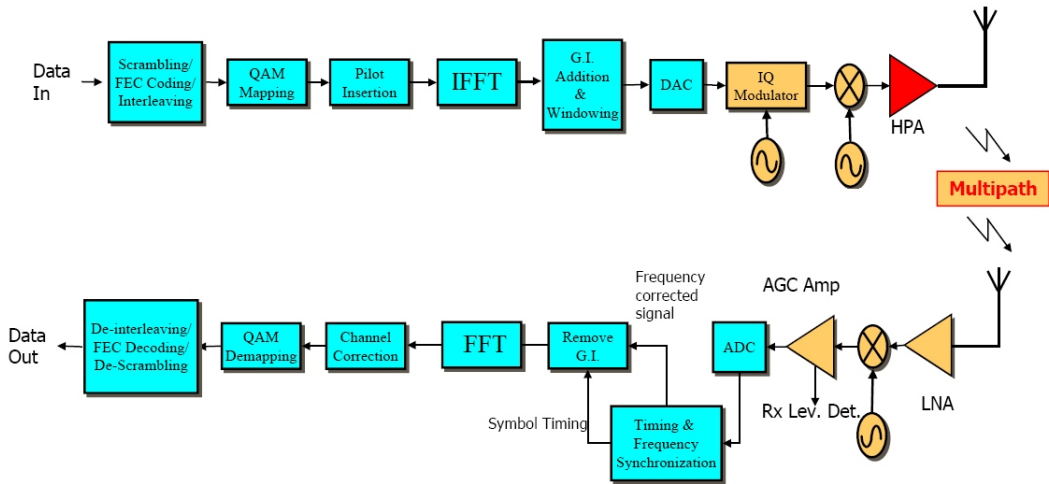


Figure 2.3: General structure of OFDM system

In general case, an OFDM signal can be defined as,[12]

$$x(t) = \sum_{i=0}^{K-1} a_i e^{j\frac{2\pi i t}{T}} s(t), 0 \leq t \leq T \quad (2.2)$$

where  $a_i$  denotes the complex valued symbol modulating the  $i^{th}$  carrier,  $s(t)$  is the time window function defined in the interval  $[0, T]$ ,  $K$  is the number of subcarriers and  $T$  is the OFDM symbol duration. As seen from Eqn.2.2, the individual subcarriers are spaced  $\Delta f=1/T$  apart.

The correlation coefficient between subcarriers can be evaluated as,

$$\rho_{xy} = \frac{1}{T} \int_0^T e^{j\frac{2\pi xt}{T}} e^{-j\frac{2\pi yt}{T}} dt \quad (2.3)$$

$$= \begin{cases} 1 & \text{if } x = y \\ 0 & \text{if } x \neq y \end{cases} \quad (2.4)$$

Therefore, different subcarriers are mutually orthogonal in the symbol interval. This property is used for demodulating the OFDM signals. For the sake of simplicity, let us assume that  $s(t)$  is a rectangular function with magnitude 1. Then, the demodulation for subcarrier- $x$  is performed as follows,

$$\frac{1}{T} \int_0^T e^{-j\frac{2\pi xt}{T}} \left[ \sum_{i=0}^{K-1} a_i e^{j\frac{2\pi it}{T}} \right] dt = \sum_{i=0}^{K-1} a_i \frac{1}{T} \int_0^T e^{j\frac{2\pi(i-x)t}{T}} dt \quad (2.5)$$

$$= \begin{cases} a_x & \text{if } i = x \\ 0 & \text{if } i \neq x \end{cases} \quad (2.6)$$

If  $s(t)$  is not chosen as a rectangular pulse shape, than  $s(t)$  should be selected so that there is no intercarrier interference (ICI), which causes loss of orthogonality between subcarriers in demodulation.

The spectrum of OFDM symbol is expressed as,

$$X(f) = FT\{x(t)\} = \sum_{i=0}^{K-1} a_i \int_{-\infty}^{\infty} e^{-j2\pi ft} e^{j\frac{2\pi it}{T}} s(t) dt \quad (2.7)$$

$$= \sum_{i=0}^{K-1} a_i S\left(f - \frac{i}{T}\right). \quad (2.8)$$

Here,  $S(f)$  is the Fourier transform of  $s(t)$ . In order to demodulate the  $x^{th}$  subcarrier, the OFDM receiver essentially samples the frequency spectrum at subcarrier frequency  $x/T$ . So, for the elimination of ICI,  $S(f)$  should satisfy the following equation:

$$S\left(\frac{x-i}{T}\right) = \begin{cases} 1 & \text{if } i = x \\ 0 & \text{if } i \neq x \end{cases} \quad (2.9)$$

Hence,

$$\frac{1}{T} \int_0^T x(t) e^{-j \frac{2\pi x t}{T}} dt = \frac{1}{T} X\left(\frac{x}{T}\right) \quad (2.10)$$

$$= \frac{1}{T} \sum_{i=0}^{K-1} a_i S\left(\frac{x-i}{T}\right) \quad (2.11)$$

$$= \begin{cases} a_x/T & \text{if } i = x \\ 0 & \text{if } i \neq x \end{cases} . \quad (2.12)$$

For  $S(f)$ ,  $\text{sinc}(fT)$  is the simplest choice, and this yields a rectangular time window. The practical problem of this is the high out of band radiation, because the tails of  $S(f)$  decrease only inversely proportional with  $f$ . In order to reduce the out of band radiation, a raised cosine time window can be employed. The advantage of the raised cosine is that the tails of the spectrum decay as  $1/f^3$  which considerably reduces the out of band radiation [12].

### 2.1.3 APPLICATIONS OF OFDM

Especially after 90's, OFDM has been selected as the transmission and multiplexing technique for a variety of applications involving terrestrial digital audio and video broadcasting and high speed wireless data transmission. In this section, some of the important applications of OFDM will be briefly discussed.

#### 2.1.3.1 DIGITAL AUDIO BROADCASTING (DAB)

DAB is the successor of current analog audio broadcasting based on AM and FM, and offers improved sound quality comparable to CD quality in addition to higher spectrum efficiency. DAB was standardized in 1995 by the European Telecommunications Standards Institute (ETSI) as the first standard to use OFDM.

DAB has four transmission modes using different sets of OFDM parameters, which are listed in Table 2.1([12]). The parameters for modes I to III are optimized for use in specific frequency bands while mode IV was introduced to provide a better coverage range at the cost of an increased vulnerability to Doppler shift.

Table 2.1: DAB OFDM parameters

	Mode I	Mode II	Mode III	Mode IV
Number of subcarriers	1536	384	192	768
Subcarrier spacing	1 kHz	4 kHz	8 kHz	2 kHz
Symbol time	1.246 ms	0.3115 ms	0.1558 ms	0.623 ms
Guard time	0.246 ms	0.0615 ms	0.0308 ms	0.123 ms
Carrier Frequency	<375 MHz	<1.5 GHz	<3 GHz	<1.5 GHz
Transmitter Separation	<96 km	<24 km	<12 km	<48 km

### 2.1.3.2 TERRESTRIAL DIGITAL VIDEO BROADCASTING (DVB-T)

In Europe, based on the successful results from the DAB field trials and measurements, terrestrial digital video broadcasting which uses OFDM was standardized by ETSI in 1996. Table 2.2 ([21]) shows the two modes defined in the DVB-T. In 1998, the DVB-T was first adopted in the United Kingdom, with multifrequency network use, 2k mode, 64 QAM, 7  $\mu$ s guard interval,  $R_c=2/3$  convolutional code and 24.13 Mbps information transmission rate.

Table 2.2: DVB-T parameters

Parameter Mode	2k	8k
Bandwidth	7.61 MHz	7.61 MHz
Number of subcarriers	1705	6817
Modulation	QPSK/16QAM	16QAM/64QAM
Symbol length	224 $\mu$ s	896 $\mu$ s
Subcarrier separation	4.464 kHz	1.116 kHz
Required SNR	3.1 dB	20.1 dB

### 2.1.3.3 IEEE 802.11 WIRELESS LAN STANDARD

Since the beginning of 90's, wireless local area networks (WLAN) for 900 MHz, 2.4 GHz, and 5 GHz ISM (Industrial, Scientific and Medical) bands have been available based on proprietary techniques. In 1997, the Institute of Electrical and Electronics Engineers (IEEE) approved an international interoperability standard. This standard specifies medium access control (MAC) procedures and three different physical layers (PHY). Two of the specified PHY's are radio-based using 2.4 GHz band and the third uses infrared light. All PHY's supported a data rate of 1 Mbps and optionally 2 Mbps.

User demand for higher data rates has spurred the development of a higher speed extension to 802.11 standard. In July 1998, the IEEE 802.11 standardization group decided to select OFDM as the basis for their new 5 GHz standard, called IEEE 802.11a, targeting a range of data rates from 6 Mbps to 54 Mbps. This new standard is the first one which uses OFDM in packet based high speed data communications. Following the IEEE 802.11 decision, ETSI BRAN HIPERLAN Type II and MMAC also adopted OFDM for their physical layer standards. Table 2.3 ([21]) lists the main parameters of IEEE 802.11a OFDM physical layer.

Table 2.3: IEEE 802.11a parameters

Channel Spacing	20 MHz
Bandwidth	16.56 MHz (-3 dB)
Number of subcarriers	52
Modulation	BPSK/QPSK/16QAM/64QAM
Symbol length	3.2 $\mu$ s
Subcarrier separation	312.5 kHz

#### 2.1.4 ADVANTAGES AND DISADVANTAGES OF OFDM

The OFDM transmission scheme has the following key advantages:

- OFDM is an efficient way to deal with multipath. For a given delay spread, the implementation complexity is significantly lower than that of a traditional single carrier system with an equalizer.
- In relatively slow time-varying channels, it is possible to enhance capacity significantly by adapting the data rate per subcarrier according to the signal to noise ratio of that particular subcarrier.
- OFDM is robust against narrowband interference because such interference affects only a small percentage of the subcarriers.

On the other hand, OFDM has also some drawbacks:

- OFDM is sensitive to frequency offset, time offset and phase noise.
- OFDM has a large peak-to-average-power ratio, which reduces the power efficiency of the radio frequency amplifier.

## 2.2 ORTHOGONAL FREQUENCY DIVISION MULTIPLE ACCESS (OFDMA)

In Section 2.1, we discussed the OFDM as a multiplexing scheme that provides better spectral efficiency and immunity to multipath fading. These advantages can also be extended to multiple-access schemes by assigning a subset of tones (subcarriers) of OFDM to individual users. The allocation of subsets of tones to various users allows for simultaneous transmission of data from multiple users, allowing for sharing the medium. In this way, it is equal to ordinary FDMA; however, OFDMA avoids the relatively large guard bands that are necessary in FDMA to separate different users.

Figure 2.4 shows the difference between the OFDM and OFDMA systems in terms of subcarrier allocation policy. In the figure, each color represents different users and as shown in the figure, at a specific timeslot OFDM systems assign all their subcarriers to only one user. On the other hand, OFDMA systems can assign each subcarrier to different users at the same time. The ability to assign the subcarriers to different users gives an opportunity to the system to choose the user who has the best channel condition at that specific subchannel. So, OFDMA system increases its capacity relative to OFDM systems. Many different policies can be used to select the proper user for each subcarriers, but each policy has different impact on system performances such as throughput, delay, fairness, etc. So, selecting the subcarrier allocation policy becomes an important issue for the systems. In our thesis, we investigate many algorithms and at the end we offer our own algorithm to select users to subcarriers considering some criteria which are all explained in detail in Section 3, 4 and 5.

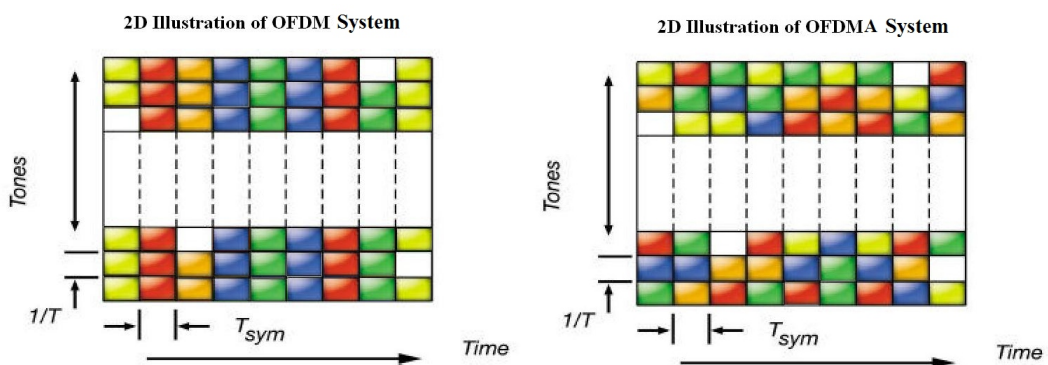


Figure 2.4: Comparison of OFDM and OFDMA Systems

Flexibility property of OFDMA is very important especially for multiple access systems.

IEEE 802.16a and IEEE 802.16e standards which are the most popular standards related with Wireless Metropol Area Networks (WMAN), prefer OFDMA technique. In the following section, we give some information about IEEE 802.16e and its parameters.

**2.2.1 IEEE 802.16e WIRELESS MAN STANDARD**

IEEE 802.16-2004 standard was built from the ground up to support broadband data connectivity for the fixed environment. This standard was primarily developed to solve broadband backhaul connectivity issue as well as to provide quickly deployable hot spot coverage and to accomodate unserved areas in a cost effective and logistic friendly manner, but it did not support any mobility requirements. In December 2002, a working group was formed under the premise of IEEE 802.16e to include mobility to complement the offerings of the IEEE 802.16a system below 6 GHz of the spectrum. The final version of IEEE 802.16e was retified and published in December 2005. Since the IEEE 802.16 family of standards deals only with the PHY and Medium Access Control (MAC) layers and does not provide the end-to-end system specifications and device interoperability requirements, the WiMAX Forum was formed to bridge this gap. WiMAX forum was formed to establish interoperability requirements and to promote industry-wide collaboration to reduce the cost of IEEE 802.16e-compliant devices and to allow deployment of services. It is envisioned that WiMAX in the WMAN context would play a role similar to that of Wi-Fi in WLAN's.

Table 2.4 gives some parameter values of IEEE 802.16e standard [33].

Table 2.4: IEEE 802.16e parameters

FFT Size	128	512	1024	2048
Channel Bandwidth	1.25 MHz	5 MHz	10 MHz	20 MHz
Sampling Frequency	1.4 MHz	5.6 MHz	11.2 MHz	22.4 MHz
Subcarrier Freq. Spacing	10.94 kHz	10.94 kHz	10.94 kHz	10.94 kHz
Useful Symbol Time	91.4 $\mu$ s	91.4 $\mu$ s	91.4 $\mu$ s	91.4 $\mu$ s
Guard Time	11.4 $\mu$ s	11.4 $\mu$ s	11.4 $\mu$ s	11.4 $\mu$ s
OFDMA Symbol Duration	102.9 $\mu$ s	102.9 $\mu$ s	102.9 $\mu$ s	102.9 $\mu$ s

## CHAPTER 3

### SYSTEM MODEL AND PROBLEM FORMULATION

#### 3.1 SYSTEM MODEL

Throughout our studies, we consider a downlink single-hop OFDMA system composed of one base station and  $N$  users (queues). Each user has an infinite buffer to store the data packets that can not be immediately transmitted. Fixed-sized packets are transmitted from base station to users via  $K$  OFDM subcarriers (servers). The system is time slotted and at the beginning of each timeslot, the assignment of servers to users is instantaneous and made by a centralized resource manager. The resource manager has perfect knowledge of the current queue backlogs and the connectivities which are assumed to be constant during a timeslot but varying independently over timeslots (e.g. block fading model). We do not allow sharing of any subcarriers and assume no error in transmission. The basic block diagram of the system is given in Figure 3.1.

The following notations are used throughout the thesis. Subscript  $i$  denotes specific sub-carrier/server, subscript  $j$  denotes specific user/queue. We use smallcase boldfaced letters without any subscription for vectors and capitalized boldfaced letters for matrices.

- $\mathbf{a}(n) = (a_1(n), a_2(n), \dots, a_N(n))$  is the vector and  $a_j(n)$  is the number of packet arrivals to queue  $j$  during time  $n$ . (The new packet arrivals at time  $n$  can be served only at time  $n + 1$  or after)
- $\mathbf{b}(n) = (b_1(n), b_2(n), \dots, b_N(n))$  is used as the vector of queue occupancies at the beginning of time  $n$ . In other words,  $b_j(n)$  is the number of packets in the User- $j$ 's buffer at the beginning of time  $n$ .

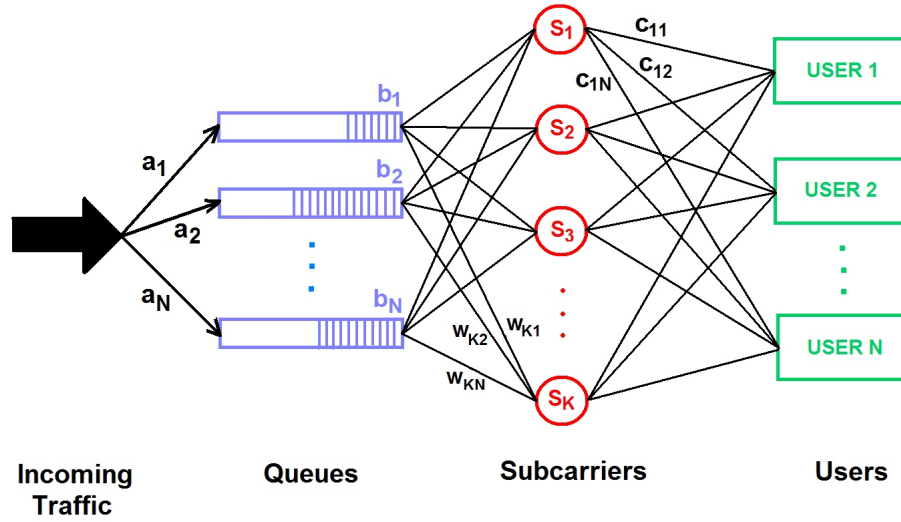


Figure 3.1: Block Diagram of the System

- $\mathbf{H}(\mathbf{n}) = \{h_{ij}(n)\}$  is the  $K$ -by- $N$  channel gain matrix at time  $n$  where  $h_{ij}(n)$  represents the channel gain which is Rayleigh distributed for subcarrier  $i$  and user  $j$ .
- $\mathbf{C}(\mathbf{n}) = \{c_{ij}(n)\}$  is the  $K$ -by- $N$  channel connectivity matrix at time  $n$  where  $c_{ij}(n)$  denotes the maximum number of packets that subcarrier  $i$  can serve from queue  $j$ .
- $\mathbf{W}(\mathbf{n}) = \{w_{ij}(n)\}$  is the  $K$ -by- $N$  allocation matrix at time  $n$  where  $w_{ij}(n)$  is equal to 1 if subcarrier  $i$  is assigned to queue  $j$ , otherwise it is equal to 0.
- $\mathbf{W}(\mathbf{b}(\mathbf{n}), \mathbf{C}(\mathbf{n}))$  is the set of all non-idling allocation matrices at time  $n$ .
- $(\mathbf{b}(\mathbf{n}), \mathbf{C}(\mathbf{n}))$  represents the state of the system at time  $n$ .

### 3.1.1 INCOMING PACKET TRAFFIC MODEL

As explained in Section 3.1, throughout the study we consider a time-slotted system. In this system, each user receives some number of packets at each slot and these packets are stored by the base station until they are transmitted to related users. The packet arrival events are illustrated in Figure 3.2 with dots. The packet arrival events are independent and identically distributed in time and among users.

It is considered that Poisson process can fit our incoming packet traffic model. Poisson distribution is a discrete probability distribution that expresses the probability of a number of events occurring in a fixed period of time if these events occur with a known average rate and independently of the time since the last event. So, for each user, we assume to characterize the incoming packet traffic model as a homogenous Poisson process with mean rate  $\lambda_i (i = 1, 2, \dots, N)$ .

In the remainder of this section, we will describe the homogenous Poisson process and give some properties related to our study.

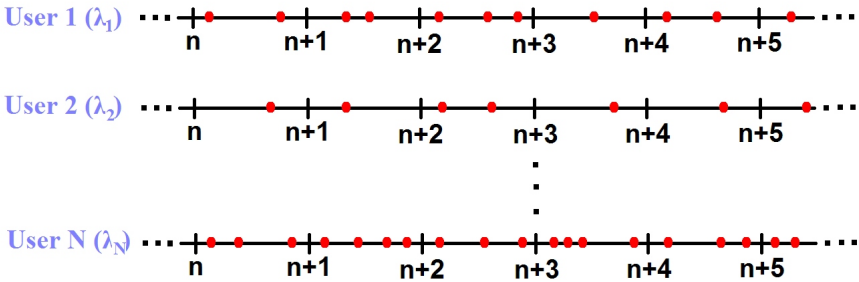


Figure 3.2: Packet Arrivals For Each User

**Definition 3.1.1** (*Counting Process*) : A stochastic process  $N(t)$  is a counting process if  $N(t) < 0$  for  $t < 0$  and  $N(t)$  is integer valued and non-decreasing with time. ([13])

Let  $N(t)$  be the counting process and gives the number of events that have occurred in the interval  $(0, t]$ . Let the event A denote the occurrence of exactly one event in the interval  $(t, t + h]$ . Similarly, let B and C denote the occurrence of none and more than one events in the same interval. Let  $P[A] = p(h)$ ,  $P[B] = q(h)$  and  $P[C] = k(h)$ .

**Definition 3.1.2**  $N(t)$  forms a Poisson process of rate  $\lambda$ , provided the following four conditions are met ([14]):

1.  $N(0) = 0$ .
2. Events occurring in nonoverlapping intervals of time are mutually independent.

3. Probabilities  $p(h)$ ,  $q(h)$  and  $k(h)$  depend only on the length  $h$  of the interval and not on the time origin  $t$ .

4. For sufficiently small values of  $h$ , we can write (for some positive constant  $\lambda$ ):

$$\begin{aligned}
 p(h) &= P[\text{one event in the interval } (t, t+h)] = \lambda h + o(h) \\
 q(h) &= P[\text{no events in the interval } (t, t+h)] = 1 - \lambda h + o(h) \\
 k(h) &= P[\text{more than one event in the interval } (t, t+h)] = o(h)
 \end{aligned}$$

where  $o(h)$  denotes any quantity having an order of magnitude smaller than  $h$ ,

$$\lim_{h \rightarrow 0} \frac{o(h)}{h} = 0 \tag{3.1}$$

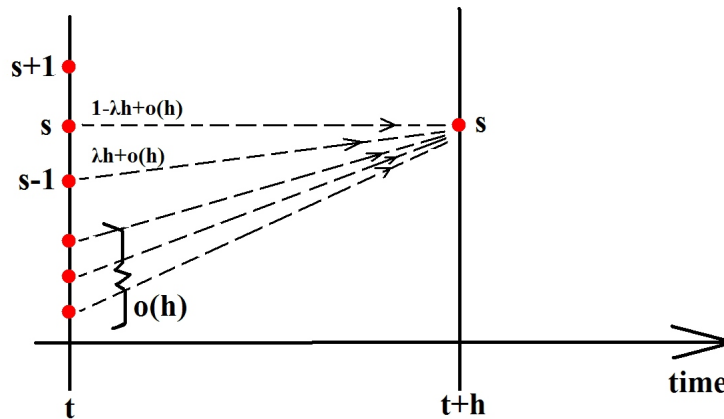


Figure 3.3: State Transition of the Poisson Process

In [13], [14] and [15], it is proved that the expected value of Poisson process is

$$E[N(t)] = \lambda t \tag{3.2}$$

and probability of  $s$  events occurring in time interval  $(0, t]$  can be calculated by using the formula given below :

$$P[N(t) = s] = e^{-\lambda t} \frac{(\lambda t)^s}{s!}, s > 0. \tag{3.3}$$

As  $t$  approaches infinity,  $E[N(t)/t]$  approaches  $\lambda$ . In other words,  $N(t)/t$  converges to  $\lambda$  as  $t$  approaches infinity. Because of this, the parameter  $\lambda$  can be also called the “arrival rate” of the Poisson process.

In our model, first we discretize time  $t$  (Poisson Random Traffic Generator time) so that the smallest discretized unit corresponds to a single “trial” for which the probability of event occurred equals  $\lambda$ . At the end of the generator time, we obtain a number which has a Poisson characteristic and has an expected value of  $\lambda.d$  where  $d$  is the number of trials. As explained above,  $d$  should go to infinity in order to obtain an ideal Poisson process, however it is impossible in real world. So we choose a finite, big enough value for  $d$  such that the process characteristic is still like Poisson. Then, per each user we specify  $\lambda_i$  values ( $i = 1, 2, \dots, N$ ) according to some parameters and conditions which will be explained in detail in Section 5.1.4. The parameter  $\lambda_i$  is chosen as a constant with respect to time and this is the reason why it is called “homogenous” Poisson process.

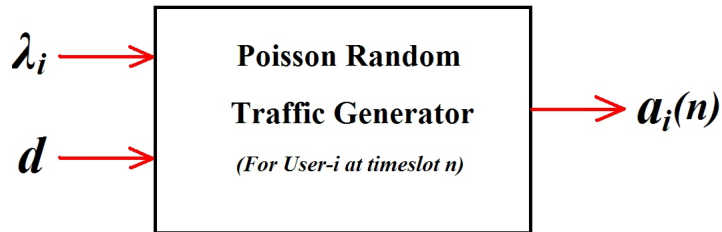


Figure 3.4: Poisson Random Traffic Generator

### 3.1.2 CHANNEL MODEL

In urban areas, the transmitted electromagnetic waves mostly do not arrive at the receiver antenna over the direct path. Moreover, due to reflections from buildings, from the ground and from other obstacles with vast surfaces, as well as scattering from trees and other scatterers, a multitude of partial waves arrive at the receiver antenna from different directions (See Figure 3.5). This effect is called as “multipath propagation”([16]). Due to multipath propagation, the received partial waves increase or weaken each other, depending on the phase relations of the waves. As a result, the received electromagnetic field strength and, thus, also the the received signal are both strongly fluctuating functions of the receiver’s position or, in case of a moving receiver, strongly fluctuating functions of time.

If the propagation delay differences among the scattered signal components at the receiver are negligible compared to the symbol interval, then the channel is said to be “frequency non-

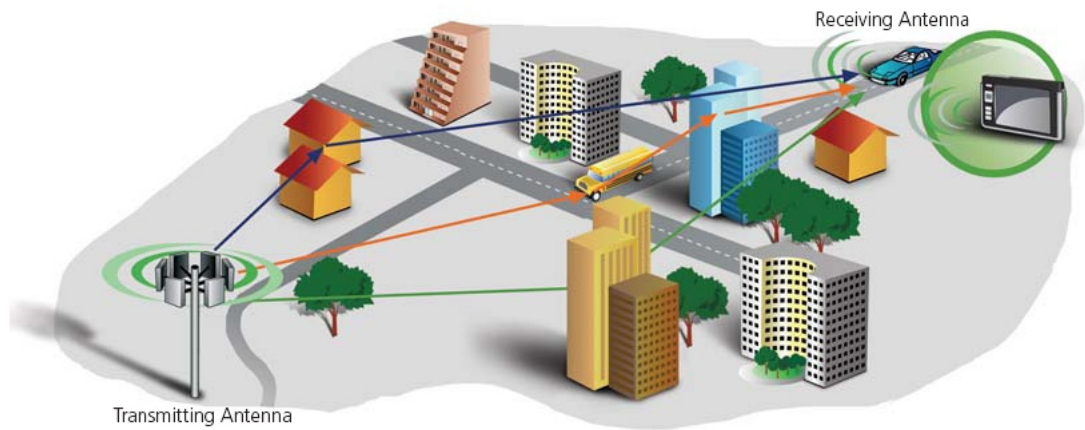


Figure 3.5: Multipath Propagation [20]

selective”, in other words “flat”. In this case, the fluctuations of the received signal can be modelled by multiplying the transmitted signal with an appropriate stochastic model process. After extensive measurements of the envelope of the received signal ([17], [18], [19]) in urban and suburban areas, i.e. in regions where the line-of-sight component is often blocked by obstacles, the Rayleigh process was suggested as the stochastic process model. Because of this, in our system model, we assume that each subcarrier (subchannel) has a flat fading which can be modeled by a Rayleigh fading process.

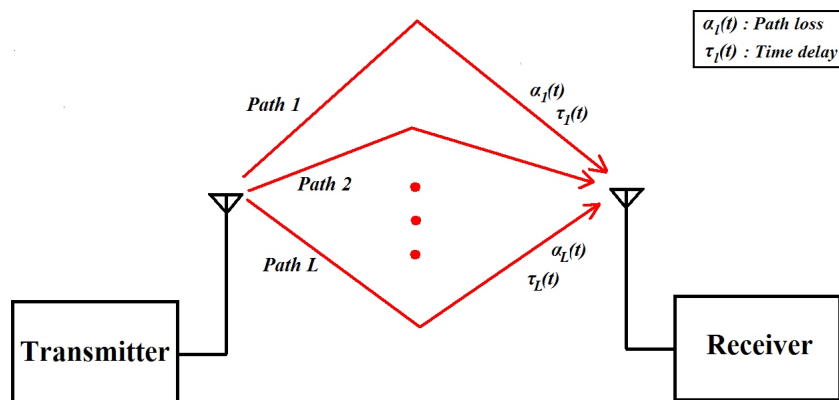


Figure 3.6: Multipath Block Diagram

Figure 3.6 shows a typical multipath fading channel often encountered in wireless communi-

cations, where there are  $L$  paths. Assume that the transmitted signal is given by :

$$x(t) = \text{Re}[s(t)e^{j2\pi f_c t}] \quad (3.4)$$

where  $s(t)$  is the equivalent baseband form of  $x(t)$  and  $f_c$  is a carrier frequency. Through the multipath fading channel, the received signal is written as:

$$y(t) = \sum_{l=1}^L \alpha_l(t)x(t - \tau_l(t)), \quad (3.5)$$

$$= \text{Re} \left[ \sum_{l=1}^L \alpha_l(t) e^{-j2\pi f_c \tau_l(t)} s(t - \tau_l(t)) e^{j2\pi f_c t} \right]. \quad (3.6)$$

where  $\alpha_l(t)$  and  $\tau_l(t)$  are the complex-valued channel loss (or gain) and real-valued time delay for the  $l^{\text{th}}$  path, both of which can be modeled as stochastic process. Then, the equivalent baseband form of  $y(t)$  is written as:

$$r(t) = \sum_{l=1}^L \alpha_l(t) e^{-j2\pi f_c \tau_l(t)} s(t - \tau_l(t)), \quad (3.7)$$

$$= \int_{-\infty}^{+\infty} h(\tau; t) s(t - \tau) d\tau. \quad (3.8)$$

where  $h(\tau; t)$  is the equivalent baseband impulse response of the multipath fading channel at instant  $t$ , which is given by:

$$h(\tau; t) = \sum_{l=1}^L \alpha_l(t) e^{-j2\pi f_c \tau_l(t)} \sigma(t - \tau_l(t)) \quad (3.9)$$

Now, assume that the transmitted signal is a continuous wave (CW) with frequency of  $f_c$ . In this case, if it is chosen that  $s(t) = 1$  in Eqn. 3.7, the received signal is written as:

$$r(t) = \sum_{l=1}^L \alpha_l(t) e^{-j2\pi f_c \tau_l(t)}, \quad (3.10)$$

$$= \sum_{l=1}^L \beta_l(t). \quad (3.11)$$

$$\beta_l = \alpha_l(t) e^{-j2\pi f_c \tau_l(t)} \quad (3.12)$$

where  $\beta_l(t)$  is a complex-valued stochastic process.

From Eqn. 3.10, it can be seen that the received signal is the sum of stochastic processes, so when there are a large number of paths, the central limit theorem can be applied ([21]). That is,  $r(t)$  can be modeled as a complex valued Gaussian stochastic process with its mean and

variance given by:

$$\mu_r = E[r(t)], \quad (3.13)$$

$$\sigma_r^2 = \frac{1}{2} E[r^*(t)r(t)]. \quad (3.14)$$

[21] clearly shows the steps to obtain the probability density function (p.d.f) of an envelope signal in multipath fading environment, such as:

$$p(z) = \frac{z}{\sigma_r^2} e^{-\frac{z^2+A^2}{2\sigma_r^2}} I_0\left(\frac{zA}{\sigma_r^2}\right), (z > 0) \quad (3.15)$$

where  $z = z(t) = |r(t)|$ ,  $A = |\mu_r|$  and  $I_0(x)$  is the *zero<sup>th</sup>* order Bessel function of the first kind, which is defined as:

$$I_0(x) = \frac{1}{2\pi} \int_0^{2\pi} e^{xcos\theta} d\theta \quad (3.16)$$

The p.d.f. of the envelope given by Eqn.3.15 is called the Rice distribution. Also

$$K = \frac{A^2}{2\sigma_r^2} \quad (3.17)$$

is called “the Ricean K factor”.

For any two Gaussian random variables X and Y, both has zero mean and equal variance  $\sigma^2$ , it can be shown that  $Z = \sqrt{X^2 + Y^2}$  is Rayleigh distributed and that  $Z^2$  is exponentially distributed ([22]). In our case, it is assumed that the phase of  $r(t)$  which is  $\theta(t)$  is uniformly distributed,  $r_I(t)$  which is the in-phase part of  $r(t)$  and  $r_Q(t)$  which is the quadrature part of  $r(t)$  are both zero-mean and Gaussian random variables. Then, A becomes 0 in Eqn. 3.15 and p.d.f. of  $z$  is given by:

$$p(z) = \frac{z}{\sigma_r^2} e^{-\frac{z^2}{2\sigma_r^2}}, (z > 0) \quad (3.18)$$

The p.d.f. of the envelope given by Eqn. 3.18 is called Rayleigh distribution that is what we are interested in this thesis. Rayleigh distribution graphic is shown in Figure 3.7 when  $\sigma^2$  is equal to 1.

As explained at the beginning of this section, if there exists a flat fading, then the fluctuations of the received signal can be modelled by multiplying the transmitted signal with an appropriate stochastic process which is Rayleigh in our thesis. Let’s call this Rayleigh generated “channel gain” as  $h_{ij}(n)$  which corresponds to user  $j$  at subcarrier  $i$  and timeslot  $n$ .  $h_{ij}(n)$  is linearly proportional to the signal SNR value when signal and noise are constant. By using this proportionality, in the next section (Section 3.1.3), the channel gain  $h_{ij}(n)$  will be mapped

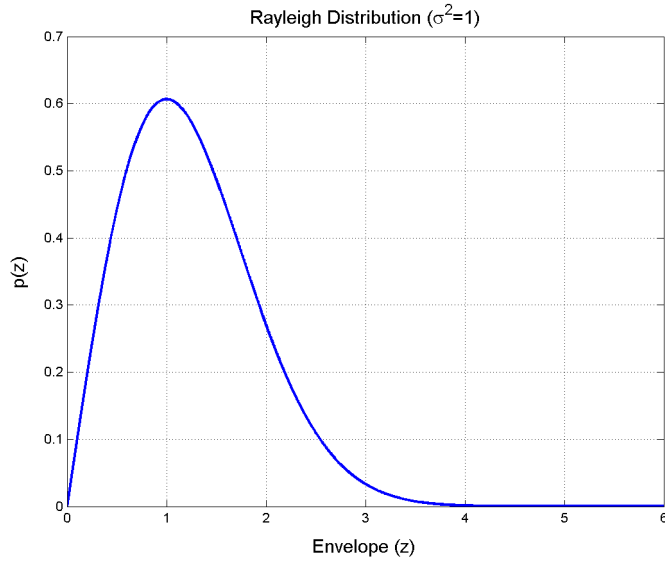


Figure 3.7: Rayleigh Distribution Graphic

to the number of packets per slot,  $c_{ij}(n)$ , which gives the maximum number of packets that subcarrier  $i$  can serve from queue  $j$ .

### 3.1.3 CONSTRUCTION CRITERIA OF CHANNEL CONNECTIVITY MATRIX

Recently, new OFDM or OFDMA systems, such as IEEE.802.11a and IEEE.802.16e, prefer to use “Adaptive Modulation” techniques in order to use the channels more efficiently. Although adaptive transmission was first investigated in the late sixties and early seventies ([23],[24]), interest in these techniques was short-lived, perhaps due to hardware constraints, lack of good channel estimation techniques, etc. As technology evolved these challenges become less constraining, so now many wireless systems, including both GSM and CDMA cellular systems as well as wireless LAN ([22]), use adaptive transmission techniques.

Adaptive modulation enables robust and spectrally efficient transmission over time-varying channels. The main idea is to estimate the channel at the receiver and feed this estimate back to the transmitter, so that the transmission scheme can be adapted relative to the channel characteristics. Systems that do not adapt their modulation to fading conditions require a fixed link margin to keep acceptable performance when the channel quality is poor. Since Rayleigh fading can cause a signal power loss up to 30 dB, designing for the worst case

channel conditions can result in very inefficient utilization of the channel. Adapting to the channel fading can increase average throughput, reduce required transmit power, or reduce average probability of bit error by taking advantage of favorable channel conditions to send at higher data rates or lower power, and by reducing the data rate or increasing power as the channel degrades. There are many adaptive techniques and most popular of them are as follows ([22]):

- Variable-rate techniques
- Variable-power techniques
- Variable error probability
- Variable-coding techniques
- Hybrid techniques

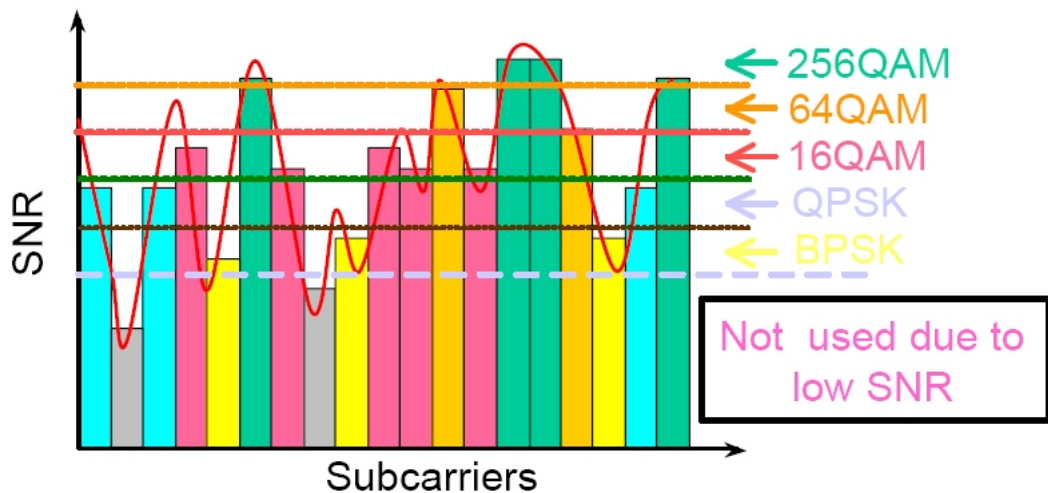


Figure 3.8: Typical Adaptive Modulation Scheme

We use the fact that there is only a very small loss of channel capacity if a white power spectrum is used (i.e. each subcarrier receives equal power) instead of the optimum power spectrum ([25]) and we decide to be only interested in variable-rate technique in our system model. In variable rate modulation, the data rate is varied relative to the received signal SNR value. This can be done by fixing the symbol rate of the modulation and using multiple

modulation schemes or constellation sizes, or by fixing the modulation and changing the symbol rate. In practice, symbol rate variation is difficult to implement because a varying signal bandwidth is impractical and complicates bandwidth sharing. So, also considering new technologies, we decide to fix the symbol rate and use multiple modulations. In our system, we are not interested in changing the coding rate according to SNR level.

Figure 3.8 shows a typical adaptive modulation scheme by also indicating the required SNR levels for different modulations. There are different standards and criteria for the SNR levels in different type of applications, so in our study, we make our own assumptions for the required SNR levels. As explained in Section 3.1.2, the channel gain  $h_{ij}(n)$ , which is proportional to SNR value, is chosen randomly by using Rayleigh fading process. So rather than discretizing SNR value directly, we prefer to discretize  $h_{ij}(n)$  in order to decide which modulation is suitable. This assumption does not effect the generalization of our results to be obtained at the end of the study.

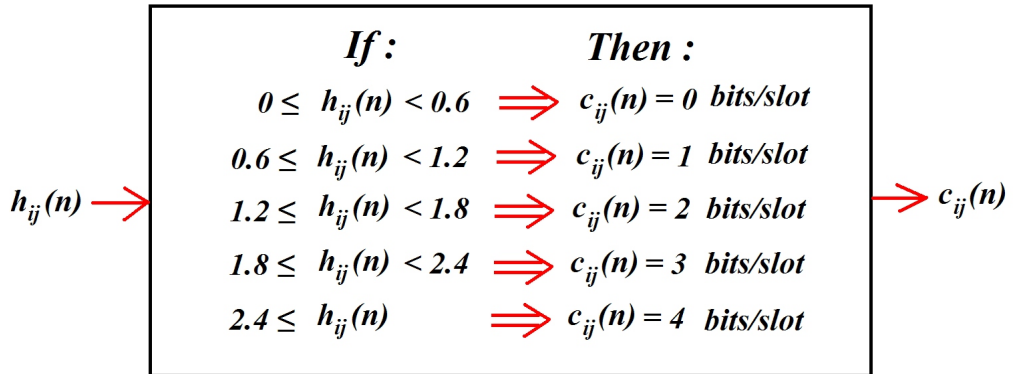


Figure 3.9: Adaptive Modulation Mapper Block Diagram

As shown in Figure 3.9, the channel gain  $h_{ij}(n)$  is mapped to the channel connectivity  $c_{ij}(n)$  which gives the maximum number of packets that subcarrier  $i$  can serve from queue  $j$ . Now, consider our system model : at time  $n$ , channel gain matrix  $\mathbf{H}(n)$  is created such that each member of  $\mathbf{H}(n)$ ,  $h_{ij}(n)$ , is generated randomly by using Rayleigh distribution with  $\sigma^2$  equal to 1. Later,  $\mathbf{H}(n)$  is converted to  $\mathbf{C}(n)$  immediately. The probability of the occurrence of each channel connectivity values ( $c_{ij}(n) \in 0, 1, 2, 3, 4$ ) can be calculated with the help of Rayleigh characteristic given in Figure 3.10.

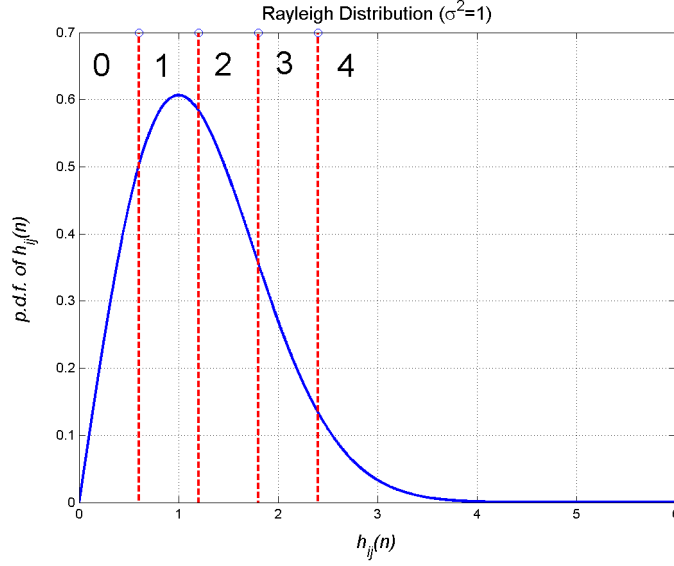


Figure 3.10: Adaptive Modulation Limits on Rayleigh Graph

Now define the probability that  $c_{ij}(n)$  is equal to  $m$ , when  $\sigma^2$  is 1:

$$P(c_{ij}(n) = m) = \int_{m_1}^{m_2} x e^{-\frac{x^2}{2}} dx, \quad (3.19)$$

Table 3.1 shows the results of the integral operation which correspond to decision criteria bounds represented as  $m_1$  and  $m_2$  for lower and upper bound respectively. According to this table, for example  $c_{ij}(n)$  has the probability of 28.89% to be assigned as “2”.

Table 3.1: Probability of the occurrence of each channel connectivity value

$m$	$m_1$	$m_2$	Probability
0	0	0.6	0.1647
1	0.6	1.2	0.3485
2	1.2	1.8	0.2889
3	1.8	2.4	0.1418
4	2.4	$\infty$	0.0561

### 3.1.4 CONSTRUCTION CRITERIA OF ALLOCATION MATRIX

Allocation matrix  $\mathbf{W}(\mathbf{n})$  is the matrix that tells us which subcarrier is assigned to which user. Generating allocation matrix is one of the most critical part of the system performance in

terms of different types of criteria such as throughput, delay. As stated in [26], there exist two important definitions for allocation matrix.

**Definition 3.1.3** Assume that at the beginning of time slot  $n$ , the state of the system is  $(\mathbf{b}(n), \mathbf{C}(n))$ . An  $K$ -by- $N$  allocation matrix  $\mathbf{W}(n) = \{w_{ij}(n)\}$  is a **feasible allocation** for time slot  $n$  if:

- (a)  $c_{ij}(n) = 0 \Rightarrow w_{ij}(n) = 0$ ,
- (b)  $\sum_{j=1}^N w_{ij}(n) \leq 1, \forall i = 1, 2, \dots, K$ .

**Definition 3.1.4** A feasible allocation matrix  $\mathbf{W}(n) = \{w_{ij}(n)\}$  is called **non-idling feasible allocation matrix**, if condition  $c$  also exists:

- (c)  $\sum_{i=1}^K w_{ij}(n)c_{ij}(n) \leq b_j(n), \forall j = 1, 2, \dots, N$ .

If  $\mathbf{W}(n)$  is a feasible allocation matrix, this means that there is no any subcarrier assignment to zero channel connectivity. Moreover, each subcarrier is assigned to at most one user. If  $\mathbf{W}(n)$  has also “non-idling” property, this means that total packets correspond to assigned subcarriers for each user is not more than the number of the user’s packets at his queue backlog.

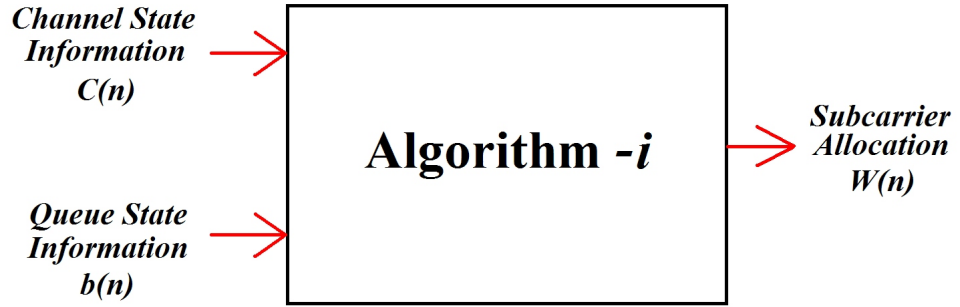


Figure 3.11: Allocation Matrix Generation Block Diagram

In Figure 3.11, the allocation matrix can be obtained by different type of algorithms all of which can have different performance measures and strategies in order to improve system performance. In Chapter 4, we explain in detail some of the subcarrier allocation algorithms

and their strategies. The main part of the study of our thesis constitute these algorithms and their effect on system performance in terms of system average throughput and system average delay.

## 3.2 PROBLEM FORMULATION

The resource allocation problem in OFDMA systems has been recently studied in different aspects, as explained in Chapter 1. In the scope of this study, we are not interested in power allocation part in order to simplify the high order complexity of the problem. Also, the fact that there is only a very small loss of channel capacity if a white power spectrum is used, support our decision about our assumption ([25]). So, in this thesis, we are interested in subcarrier allocation which can be also called “bandwidth allocation”.

Throughout our study, we focus on two important problems: 1) System average throughput maximization, and 2) System average delay minimization. In Chapter 5, we will investigate the throughput and delay performances of the algorithms explained in Chapter 4.

### 3.2.1 SYSTEM AVERAGE THROUGHPUT MAXIMIZATION PROBLEM

In the literature, there are many studies([1],[2],[3]) which are interested in system instantaneous throughput maximization. This maximization problem can be formulated as follows:

**Definition 3.2.1** Define  $\mathbf{W}(\mathbf{b}, \mathbf{C})$  as the set of all non-idling feasible allocation matrices.  $W^*(n)$  is the allocation matrix which maximizes the system instantaneous throughput at time slot  $n$ , if the condition holds given below:

$$\sum_{i=1}^K \sum_{j=1}^N c_{ij}(n) w_{ij}^*(n) \geq \sum_{i=1}^K \sum_{j=1}^N c_{ij}(n) w_{ij}(n), \forall W(n) \in \mathbf{W}(\mathbf{b}, \mathbf{C}) \quad (3.20)$$

[27] and [6] show that using the maximum instantaneous throughput policy may result in poor performance with respect to a long run throughput criterion. So, in our study, we investigate the algorithms in terms of the “system average throughput” criterion.

**Definition 3.2.2** Define  $\mathbf{W}(\mathbf{b}, \mathbf{C})$  is the set of all non-idling feasible allocation matrices. System average throughput maximization policy  $\pi$  is the subcarrier allocation policy which

chooses  $W^*$  among  $\forall W \in \mathbf{W}(\mathbf{b}, \mathbf{C})$  such that it maximizes the function  $L_T^\pi$  at the finite horizon  $T$ :

$$L_T^\pi = \sum_{n=0}^T \left[ \sum_{i=1}^K \sum_{j=1}^N c_{ij}(n) w_{ij}(n) \right] \quad (3.21)$$

### 3.2.2 SYSTEM AVERAGE DELAY MINIMIZATION PROBLEM

As well as the throughput, the packet delay issue is also a very important topic for system performance. Some applications such as VoIP, video broadcast are very sensitive to the packet delay and their service quality can be degraded proportional to the average delay.

In our study, additional to the system average throughput, we are also interested in the relative performances of the algorithms on system average delay issue.

A very well known theorem, Little's Theorem ([28]), says that minimizing the average delay is the same as minimizing the average backlog (queue size). So, when considering delay performance, we investigate the average queue sizes in our thesis. The theorem and also its proof is given in A.

After the Little's Theorem, now we can formulate the system average delay minimization problem as follows:

**Definition 3.2.3** Define  $\mathbf{W}(\mathbf{b}, \mathbf{C})$  as the set of all non-idling feasible allocation matrices. System average delay minimization policy  $\pi$  is the subcarrier allocation policy which chooses  $W^*$  among  $\forall W \in \mathbf{W}(\mathbf{b}, \mathbf{C})$  such that it minimizes the cost function  $C_T^\pi$  at the finite horizon  $T$ :

$$C_T^\pi = \sum_{n=0}^T \sum_{j=1}^N b_j(n) \quad (3.22)$$

As seen in Definition 3.2.3, delay minimization is expressed as backlog minimization.

## CHAPTER 4

### SUBCARRIER ALLOCATION ALGORITHMS

#### 4.1 INTRODUCTION TO SUBCARRIER ALLOCATION

The dynamic transmitting/receiving activity at the base station can generally be described as follows. For  $\forall j, (j \in \{1, 2, \dots, N\})$ :

$$b_j(n+1) = [b_j(n) - \sum_{i=1}^K w_{ij}(n)c_{ij}(n)]^+ + a_j(n) \quad (4.1)$$

where  $[x]^+$  represents  $[x]^+ = \max\{0, x\}$ .

Note that in Equation 4.1, the base station can not have a control on the packet arrivals,  $\mathbf{a}(\mathbf{n})$ , and the channel characteristics,  $\mathbf{C}(\mathbf{n})$ . So, in order to achieve the desired performance (throughput, stability, e.t.c.), the base station can only have a control on the allocation matrix,  $\mathbf{W}(\mathbf{n})$ , by using the proper subcarrier allocation algorithm.

In this thesis, we evaluate some algorithms in terms of the average throughput, average delay and also complexity. Complexity issue is very important because, at the base station, the subcarrier assignment decision should be made very fast and the complexity of an algorithm is directly proportional to the decision duration. So even an algorithm performs very well, if its complexity is high, it is difficult to be used in real life because of technology and/or economic limits.

#### 4.2 BIG-O NOTATION

For describing the complexity of the algorithms, we use big-O-notation. The big-O-notation gives an idea about the upper bound of the number of calculations of an algorithm in the worst

case with respect to some parameters. In our case, the parameters are the number of users (N) and the number of subcarriers (K). Note that, the big-O expressions do not have constants or low-order terms. This is because, when the parameters get large enough, constants and low-terms don't matter. Definition 4.2.1 gives a formal definition of big-O-notation.

**Definition 4.2.1** *A function  $g(n)$  is  $O(f(n))$ , if and only if there exist positive constants  $k$  and  $n_0$  such that*

$$|g(n)| \leq k|f(n)|, \forall n \geq n_0. \quad (4.2)$$

Here are some examples of big-O calculations:

- $f(n) = 3n^2 + 2n + 5 \Rightarrow O(f(n)) = O(n^2)$
- $f(n) = \sum_{i=1}^n i = \frac{n(n+1)}{2} \Rightarrow O(f(n)) = O(n^2)$
- Assume there exist a part of a code in the algorithm as given below

```
for(i=0 ; i < K ; i++)
    for(j=0 ; j < N ; j++)
    {
        ... % assume some O(1) complexity operations exist here
    }
}
```

The inner loop, loops N times so the inner loop complexity is  $N \times O(1) = O(N)$ . The outer loop calls the inner loop K times. So the total complexity becomes  $K \times O(N) = O(KN)$ .

In the following sections (from Section 4.3 to 4.7), we introduce the algorithms which are simulated in Chapter 5. The last algorithm among 5 algorithms called “Updated Maximum Weight Matching” is proposed by us by considering average throughput, average delay, and complexity criteria.

The names of the algorithms that we choose to evaluate are given below:

- Maximum Instantaneous Throughput Algorithm (MIT)
- Load Equalizing Algorithm (LE)
- Maximum Weight Matching Algorithm (MWM)
- Recursive Maximum Weight Matching Algorithm (r-MWM)
- Updated Maximum Weight Matching Algorithm (u-MWM)

### 4.3 MAXIMUM INSTANTANEOUS THROUGHPUT ALGORITHM (MIT)

There are many papers in the literature ([1], [2], [4], [3], [29]) which focus on maximizing the instantaneous throughput. All these algorithms aim to maximize the throughput at the current time and they are not interested in the future throughput. Related with this characteristic of the algorithm, [27] and [6] show that using maximum instantaneous throughput policy can sometimes perform poorly with respect to a long run throughput criterion.

As given in Definition 3.2.1, a maximum instantaneous throughput policy  $\pi$  chooses  $W^*(n) \in \mathbf{W}(\mathbf{b}, \mathbf{C})$  at time slot  $n$ , such that

$$\sum_{i=1}^K \sum_{j=1}^N c_{ij}(n) w_{ij}^*(n) \geq \sum_{i=1}^K \sum_{j=1}^N c_{ij}(n) w_{ij}(n), \forall W(n) \in W(b, C) \quad (4.3)$$

where  $\mathbf{W}(\mathbf{b}, \mathbf{C})$  is the set of all non-idling feasible allocation matrices.

The idea of MIT is to allocate the subcarrier  $i$  to the user  $j$  with the largest  $c_{ij}$  without considering the backlogs. In our thesis, we make some modifications on the MIT algorithm in order to obtain a less complex algorithm. The algorithm, that we are interested in, has the decision mechanism at each time slot as follows:

- for  $i=1$  to  $K$ ;
  - choose  $j^* = \operatorname{argmax}_{j \in J} c_{ij}$ , ( $j' \in J$  if  $b_{j'} \geq c_{ij}$ ),
  - if there exists more than one  $j^*$  which has the same value of  $c_{ij}$ , then choose one of them randomly,
  - $w_{ij^*} = 1$  elsewhere  $w_{ij} = 0$ ,
  - $b_{j^*} = b_{j^*} - c_{ij^*}$

- end.

As seen in the decision mechanism given above, all  $c_{ij}$  should be checked to find the all  $j^*$ 's. This activity corresponds to  $K \times N$  operations. Definition 4.2.1 says that the multipliers and lower order terms are not included for calculating big-O complexity. So, we can say that MIT has the complexity of  $O(KN)$ .

#### 4.4 LOAD EQUALIZING ALGORITHM (LE)

In Section 4.3, MIT policy which instantaneously maximizes the number of packets being served now has been introduced. In this section, LE policy, which maximizes the number of non-empty queues (hence the multiuser diversity and the number of packets served) in the future, is introduced. LE policy distributes the future workload among queues as evenly as possible in order to minimize the future expected server idling. [7] and [6] show that, in some conditions, LE becomes delay and throughput optimal. But in the general case, it should be taken into account that LB policy sacrifices the current throughput (by giving priority to longest queue) for the future throughput.

To introduce the LB policy, we use the following definitions given in [26].

**Definition 4.4.1** *Considering ordering function  $ord : R^N \rightarrow R^N$  to be such that  $\forall x \in R^N$ ,  $y = ord(x)$  has the ordered elements of  $x$  in descending order i.e.  $y_i \geq y_{i+p}$ ,  $p > 0$ .*

**Definition 4.4.2** *It is said that  $x \leq_{LQO} y$  ( $x$  is more balanced than  $y$ ) iff  $ord(x) \leq_{lex} ord(y)$  where the relation  $\leq_{lex}$  on  $R^N$  is the lexicographic (i.e. dictionary or alphabetic) ordering.*

For example  $ord(3, 4, 6, 3) = (6, 4, 3, 3)$  and  $ord(1, 0, 6, 5) = (6, 5, 1, 0)$ . Then  $ord(3, 4, 6, 3) = (6, 4, 3, 3) \leq_{lex} (6, 5, 1, 0) = ord(1, 0, 6, 5)$ .

Now we can define LE policy:

**Definition 4.4.3** *A Load Equalizing policy  $\pi$  chooses  $W^*(n) \in W(b, C)$  at time slot  $n$ , such that*

$$[b(n) - \mathbf{I}(W^*(n) \odot C(n))]^+ \leq_{LQO} [b(n) - \mathbf{I}(W(n) \odot C(n))]^+, \forall W(n) \in W(b, C) \quad (4.4)$$

where an elementwise product  $\mathbf{W} \odot \mathbf{C}$  is a matrix  $[w_{ij}c_{ij}]$ ,  $\mathbf{1}$  is a  $K$ -dimensional row vector of  $K$  ones, and finally  $[v]^+ = [v_1^+, v_2^+, \dots, v_N^+]$  with  $v_j^+ = \max\{0, v_j\}$ .

In order to obtain a less complex algorithm, we modify LE policy as follows:

- for  $i=1$  to  $K$ ;
  - choose  $j^* = \operatorname{argmax}_{j \in J} (b_j)$ , ( $j' \in J$  if  $b_{j'} \geq c_{ij'}$  and  $c_{ij'} \neq 0$ ),
  - if there exists more than one  $j^*$  which has the same value of  $(b_j)$ , then choose one of them randomly,
  - $w_{ij^*} = 1$  elsewhere  $w_{ij} = 0$ ,
  - $b_{j^*} = b_{j^*} - c_{ij^*}$ ,
- end.

The complexity calculation of LE is very similar to MIT complexity. At each subcarrier assignment,  $N$  queue lengths should be checked and the largest should be found. This operation is done  $K$  times. So, the total operation number is proportional to  $K \times N$ . Other required operations have lower order than  $O(KN)$ . Finally, we can say that LE complexity has  $O(KN)$  complexity.

#### 4.5 MAXIMUM WEIGHT MATCHING ALGORITHM (MWM)

When allocating the subcarriers, the MIT algorithm, in Section 4.3, uses only the channel state information ( $c_{ij}$ ) for making a decision. On the other hand, the LE algorithm, in Section 4.4, uses only queue state information ( $b_j$ ). However, both of these information are valuable and can be used jointly for subcarrier allocation.

[5] offers an algorithm which takes into account both of the channel state and queue state information. In addition to this, [5], [8] and [30] prove that maximum weight matching type algorithms are rate stable, in other words, average throughput optimal. Here, the important point is that all these three papers do not say anything about the delay performance of MWM.

The main idea of the MWM algorithm can be formulated as follows: A maximum weight matching policy  $\pi$  chooses  $W^*(n) \in \mathbf{W}(\mathbf{b}, \mathbf{C})$  at time slot  $n$ , such that

$$\sum_{i=1}^K \sum_{j=1}^N b_j(n) c_{ij}(n) w_{ij}^*(n) \geq \sum_{i=1}^K \sum_{j=1}^N b_j(n) c_{ij}(n) w_{ij}(n), \forall W(n) \in W(b, C) \quad (4.5)$$

where  $\mathbf{W}(\mathbf{b}, \mathbf{C})$  is the set of all non-idling feasible allocation matrices.

Looking at Equation 4.5, it seems that one has to calculate all  $b_j(n) c_{ij}(n)$  values before obtaining  $W^*(n)$ . However, [8] says that, calculating the weights subcarrier by subcarrier gives the same result as the straightforward and less computationally complex implementation.

$$\sum_{i=1}^K \sum_{j=1}^N b_j(n) c_{ij}(n) w_{ij}^*(n) = \sum_{i=1}^K \max_j (b_j c_{ij}) \quad (4.6)$$

Equation 4.6 provides an opportunity for us to make a decision subcarrier by subcarrier, independent from the other subcarriers.

Here is the decision mechanism of the implemented MWM algorithm taken from [5]:

- $\mathbf{TX} = \{TX_{1^*}, TX_{2^*}, \dots, TX_{N^*}\} = 0$ ;
- for  $i=1$  to  $K$ ;
  - choose  $j^* = \operatorname{argmax}_j (b_j c_{ij})$ ,
  - if there exists more than one  $j^*$  which has the same value of  $(b_j c_{ij})$ , then choose one of them randomly,
  - $TX_{j^*} = TX_{j^*} + c_{ij^*}$ ,
  - $w_{ij^*} = 1$  elsewhere  $w_{ij} = 0$ ,
- end
- for  $i=1$  to  $K$ ;
  - if  $TX_{j^*(i)} \geq b_{j^*(i)}$ , then  $w_{ij^*} = 0$ ,
- end.

The first loop has the complexity of  $O(KN)$  and the second loop has the complexity of  $O(K)$ . So the total complexity seems to be  $O(KN + K) = O(K(N + 1))$ . Here, the second loop complexity of  $O(K)$  does not increase the total complexity and this can be explained as follows. Assume that  $N$  is constant and  $K$  is a variable. Then  $A=N+1$  becomes constant and the total complexity becomes  $O(AK)$ . As explained at the beginning of the Chapter 4, the big-O expression does not include constant multipliers. So, the complexity becomes  $O(AK)=O(K)$ . On the other hand, assume  $K$  is constant and  $N$  is a variable. Then the complexity expression becomes  $KN + K$ . In the expression, the first  $K$  is the multiplier and the second  $K$  is the constant. Neither of these are included to the big-O notation, so the complexity becomes  $O(N)$ . As a result, the overall complexity of the algorithm can be accepted as  $O(KN)$ .

### 4.6 RECURSIVE MAXIMUM WEIGHT MATCHING (r-MWM)

In the MWM algorithm given in Section 4.5, the same backlog information ( $\mathbf{b}(n)$ ) is used during the whole subcarrier assignment decisions at time  $n$ , without updating after any subcarrier assignment to any user. Because of this, this can cause some imbalanced queues at the end of the assignment. To visualize the effect better, see the Figure 4.1.

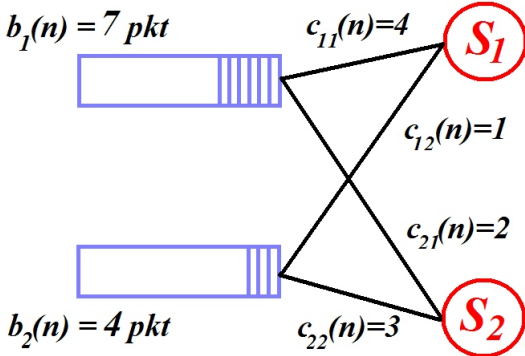


Figure 4.1: Maximum Weight Matching

First consider the MWM algorithm for the situation in Figure 4.1. For subcarrier 1,  $b_1(n)c_{11}(n) = 28 > b_2(n)c_{12}(n) = 4$  so subcarrier 1 is assigned to user-1. For subcarrier 2,  $b_1(n)c_{21}(n) = 14 > b_2(n)c_{22}(n) = 12$  so subcarrier 2 is also assigned to user-1. At the end, total transmitted packet number is 6 and final  $b(n)$  is  $b(n) = (1, 4)$ . Now consider the algorithm which

takes into account the new queue lengths after each subcarrier assignment. For subcarrier 1,  $b_1(n)c_{11}(n) = 28 > b_2(n)c_{12}(n) = 4$  so subcarrier 1 is assigned to user-1. But now the new queue size of user-1 is  $b_{1'}(n) = 3$ . For subcarrier 2,  $b_{1'}(n)c_{21}(n) = 6 < b_2(n)c_{22}(n) = 12$  so this time subcarrier 2 is assigned to User-2. At the end, this time total transmitted packet number is 7 and final  $b(n)$  is  $b(n) = (3, 1)$ . As a result, with the second algorithm we obtain larger throughput and more stable queue sizes.

[9] proposes an algorithm which has decision mechanism given below in order to avoid imbalanced queues.

- $X = \{1, 2, \dots, K\}$  ;
- Loop (until STOP)
  - If  $X = \emptyset$  then STOP ;
  - $(i^*, j^*) = \underset{j \in \{1, \dots, N\}}{\operatorname{argmax}}_{i \in X} b_j c_{ij}$  ;
  - If  $b_{j^*} c_{i^* j^*} > 0$ , then  $w_{i^* j^*}^* = 1$  else STOP ;
  - $b_{j^*} = b_{j^*} - c_{i^* j^*}$  and  $X = X - \{i^*\}$  ;
- Assign  $W^* = \{w_{ij}^*\}$  ;

In the expression, the loop stops if: 1) all subcarriers are assigned, or 2) all the queues become empty before assigning all subcarriers. For big-O expression, we have to think the worst case, so we have to consider the stop when the all subcarriers are assigned. Before the decision mechanism starts, there are  $K$  elements in  $X$ . Then the algorithm operates  $(i^*, j^*) = \underset{j \in \{1, \dots, N\}}{\operatorname{argmax}}_{i \in X} b_j c_{ij}$  line. This operation makes  $N$  calculations per each subcarrier, so the total operation number is  $K \times N$  in the first loop. In the second loop, the group number of  $X$  decreases by one, so now the total operation number becomes  $(K-1) \times N$ . This goes on until the last subcarrier is assigned. At the last loop, the total operation number becomes  $(1) \times N$ . The sum of the whole operations  $S$  is:

$$S = KN + (K - 1)N + (K - 2)N + \dots + 1N \quad (4.7)$$

$$= N [K + (K - 1) + (K - 2) + \dots + 1] \quad (4.8)$$

$$= N \left[ \frac{K(K + 1)}{2} \right] \quad (4.9)$$

$$= \frac{1}{2}NK^2 + \frac{1}{2}NK \quad (4.10)$$

As the same idea explained in Section 4.5, we can ignore the multipliers and low order terms when writing big-O expression. Finally it can be said that r-MWM algorithm has the worst case complexity of  $O(NK^2)$ .

#### 4.7 UPDATED MAXIMUM WEIGHT MATCHING (u-MWM)

From the previous studies as [5], [8] and [30], we know that maximum weight matching type algorithms have the best performance in terms of system average throughput criteria. However, this type of algorithms do not guarantee the best system average delay performance. In order to improve the system average delay performance, [8] proposes an algorithm which is explained in Section 4.6. Now, the problem becomes the complexity. As explained in previous sections, MIT, LE, MWM algorithms have  $O(KN)$  complexity, on the other hand r-MWM has  $O(K^2N)$  complexity. When the subcarrier number is large enough, this complexity difference can become an important issue. For instance, IEEE 802.16e standard uses up to 2048 subcarriers ([31]) and there can be an important decision time duration difference between MWM and r-MWM.

Considering all these effects, we propose an algorithm which has a maximum weight matching characteristic, with  $O(KN)$  complexity, and further takes into account avoiding imbalanced queues as r-MWM in order to improve the delay performance.

Our proposed algorithm is called the ‘‘Updated’’ Maximum Weight Matching, because after each subcarrier assignment, it updates the queue lengths without increasing the complexity. Here is the decision mechanism of u-MWM:

- for  $i=1$  to  $K$ ;
  - choose  $j^* = \operatorname{argmax}_{j \in J} (b_j)c_{ij}$ , ( $j' \in J$  if  $b_{j'} \geq c_{ij'}$ ),
  - if there exists more than one  $j^*$  which has the same value of  $(b_j)$ , then choose one of them randomly,
  - $w_{ij^*} = 1$  elsewhere  $w_{ij} = 0$ ,
  - $b_{j^*} = b_{j^*} - c_{ij^*}$ ,
- end.

The calculation of the complexity of u-MWM is very similar to the MIT and LE algorithm. Per each subcarrier,  $(b_j)c_{ij}$  values should be calculated (this corresponds to N operations) and the largest to be found. So, there exists KxN operations in total which means that the complexity of u-MWM is  $O(KN)$ . Other required operations has low order complexity and does not change the overall complexity.

## CHAPTER 5

### SIMULATIONS AND RESULTS

After explaining the system model in Chapter 3 and the algorithms in Chapter 4, in this chapter first we introduce our simulation environment and also explain the calculation of some important parameters used in our simulations. Later, we show the simulation results which investigate the algorithms' system average throughput performance and system average delay performance with respect to the parameters given below:

- Number of Users,  $N$
- Number of Subcarriers,  $K$
- Load,  $L$  (to be explained in Section 5.1.3)
- Balance Ratio,  $r$  (to be explained in Section 5.1.4).

#### 5.1 SIMULATIONS AND SOME RELATED PARAMETERS

##### 5.1.1 SIMULATION ENVIRONMENT

The main part of the simulation codes in our thesis are written in *BORLAND*® C++ *Builder*<sup>TM</sup> 6.0 environment. We prefer to use C++ code for our simulations because of its efficiency and also its speed. Although we use “Visual” C++, the graphical properties of this environment is not so rich. Moreover, analyzing the output data of our simulations requires more capability than C++ environment. So, throughout our study, we also use *MATLAB*® 6.5 for processing the output data obtained from simulations.

As an example, Figure 5.1 shows one of the graphical user interface in our thesis prepared in *BORLAND*® C + +.

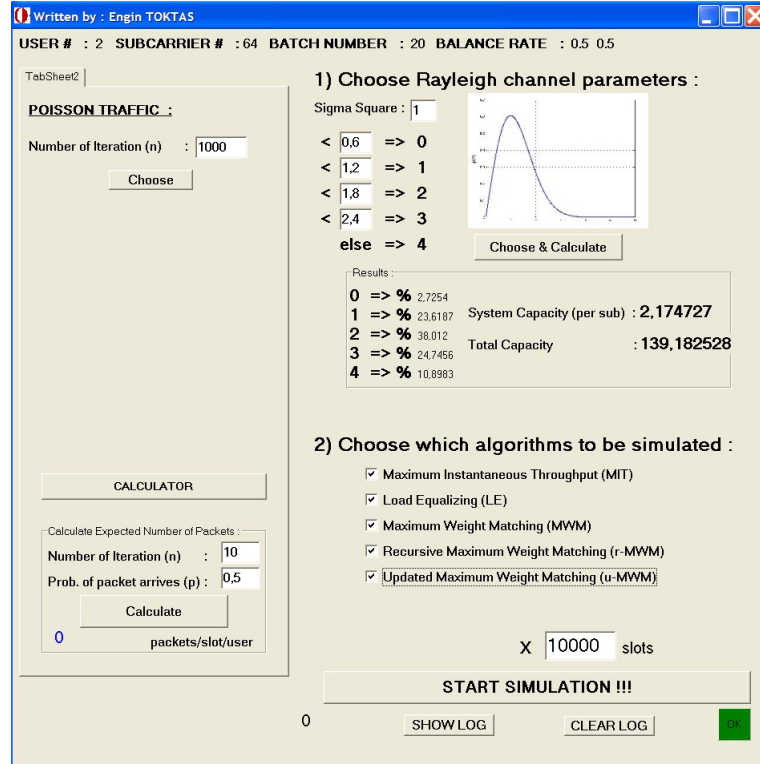


Figure 5.1: An example of the graphical user interface

## 5.1.2 SYSTEM AVERAGE THROUGHPUT AND SYSTEM AVERAGE DELAY

The simulations in this thesis are mainly done for understanding the performances of the subcarrier allocation algorithms in terms of system average throughput and system average delay. Although we mention these terms in Section 3.2.1 and 3.2.2, in this section we provide here formal definitions.

The system average throughput can be formulated as follows,

$$system\_average\_throughput = \frac{1}{T} \sum_{n=0}^{T-1} \sum_{j=1}^N \sum_{k=1}^K c_{ij}(n)w_{ij}(n) \quad (5.1)$$

The system average delay can be formulated as follows,

$$system\_average\_delay = \frac{a}{T} \sum_{n=0}^{T-1} \sum_{j=1}^N b_j(n) \quad (5.2)$$

where  $a$  is a constant and comes from the relationship between average queue size and average delay explained in Little's theorem (see Section 3.1.1). “ $a$ ” is a constant number, so when comparing the delay performances of the algorithms with each other, it is also possible to compare the average queue sizes without any loss of information. Throughout our study we prefer to use average queue sizes for investigating the delay performances.

The system average queue size can be formulated as follows,

$$system\_average\_queue\_size = \frac{1}{T} \sum_{n=0}^{T-1} \sum_{j=1}^N b_j(n). \quad (5.3)$$

### 5.1.3 CALCULATION METHOD FOR “LOAD” PARAMETER

Throughout our study, we are interested in many parameters such as the number of users, number of subcarriers, incoming packet rates per each user, etc. Here, the problem is that some parameters may effect the other parameters and this causes some difficulties to compare the results with each other. For example, if you increase the number of users without changing the number of subcarriers, system average throughput capacity increases because of the effect of “multi-user diversity”. So, for instance, light/heavy traffic definition should be modified each time according to the number of users.

In addition to expressing all our throughput and delay results in terms of “packets/slot/subcarrier”, we also use a “load” term which generally tells how close the packet input traffic density is to system average output capacity.

**Definition 5.1.1** *The load,  $L$ , is the ratio between the system average input packet rate and the system average output capacity*

$$L = \frac{\sum_{j=1}^N E\{a_j\}}{K\gamma_N}, \quad (5.4)$$

where  $E\{a_j\}$  represents average incoming packet rate (in packets/slot) of user- $j$  and  $\gamma_N$  represents average output capacity of one subcarrier when there exists  $N$  users.

In the literature, there are many ‘‘capacity’’ definitions. Rather than using those definitions, we prefer to use our own definition which is simple and easy to be calculated. Our definition does not exactly corresponds to an information theoretic or operational ‘‘capacity’’ but it gives a sufficient idea for our study about the upper bound of the system average throughput.

**Definition 5.1.2** Assume that there are  $N$  users and the queue lengths of each user are non-empty. Then, average output capacity for one subcarrier,  $\gamma_N$ , is equal to:

$$\gamma_N = E \{ \max\{c_1, c_2, \dots, c_N\} \}, \quad (5.5)$$

where  $c_j$  is the connectivity matrix element for a specific subcarrier of user  $j$  and has a statistical property given at Table 3.1.

For example, if there exists 1 user ( $N=1$ ), then the average output capacity for one subcarrier becomes:

$$\gamma_1 = E \{ \max\{c_1\} \} \quad (5.6)$$

$$= E \{ c_1 \} \quad (5.7)$$

$$= 0 * (0.1647) + 1 * (0.3485) + 2 * (0.2889) + 3 * (0.1418) + 4 * (0.0561) \quad (5.8)$$

$$= 1.5761 \text{ pkt/slot} \quad (5.9)$$

Now, let’s generalize the formula for  $N$  users. Consider a channel which is discretized at  $L+1$  levels ( $c_j \in \{0, 1, 2, \dots, l, \dots, L\}$ ) and probability of occurring each level for one user is  $p_0, p_1, \dots, p_l, \dots, p_L$  respectively. Assume that in the system, there are  $N$  users and  $c_{max,N} = \max\{c_1, c_2, \dots, c_N\}$ . Then,

$$P(c_{max,N} = 0) = (p_0)^N \quad (5.10)$$

$$P(c_{max,N} = l) = \left( \sum_{x=0}^l p_x \right) - \left( \sum_{x=0}^{l-1} p_x \right), l \in \{1, 2, \dots, L\} \quad (5.11)$$

and

$$\gamma_N = E \{ c_{max,N} \} \quad (5.12)$$

$$= \sum_{x=0}^L x \cdot P(c_{max,N} = x) \quad (5.13)$$

If we consider our channel model and its statistics given at Table 3.1, we can obtain the average output capacity per subcarrier with respect to the number of users by using 5.11 and 5.12 as shown in Table 5.1.

Table 5.1: Average output capacity (pkt/slot) per subcarrier w.r.t number of users

$N$	$P(c_{max,N} = 0)$	$P(c_{max,N} = 1)$	$P(c_{max,N} = 2)$	$P(c_{max,N} = 3)$	$P(c_{max,N} = 4)$	$\gamma_N$
1	0.1647	0.3485	0.2889	0.1418	0.0561	1.5761
2	0.0271	0.2362	0.3800	0.2476	0.1091	2.1752
4	0.0007	0.0686	0.3446	0.3799	0.2062	2.7222
8	0.0000	0.0048	0.1665	0.4588	0.3699	3.1938
32	0.0000	0.0000	0.0009	0.1568	0.8424	3.8418
64	0.0000	0.0000	0.0000	0.0248	0.9752	3.9752

We have stated so far in this section that the output capacity per subcarrier increases when the number of users increases because of the “multiuser diversity” effect. This effect can be seen very clearly in Figure 5.2. In this figure, rather than plotting the p.d.f of  $c_{max,N}$ , we plot the p.d.f characteristic of  $h_{max,N}$  which can be described as  $h_{max,N} = \max\{h_1, h_2, \dots, h_N\}$  by using the “histogram” command of MATLAB. We explained the relationship between  $c_{ij}$  and  $h_{ij}$  in Section 3.1.3. As explained in that section,  $c_{ij}$  is the discretization result of  $h_{ij}$ . So, if the mean of  $h_{ij}$  increases than the mean of  $c_{ij}$  also increases. In Figure 5.2, it can be seen that the mean of  $h_{ij}$  shifts to the right when the number of users increases. The discretization limits used for obtaining  $c_{ij}$  can also be seen in the figure as dashed lines.

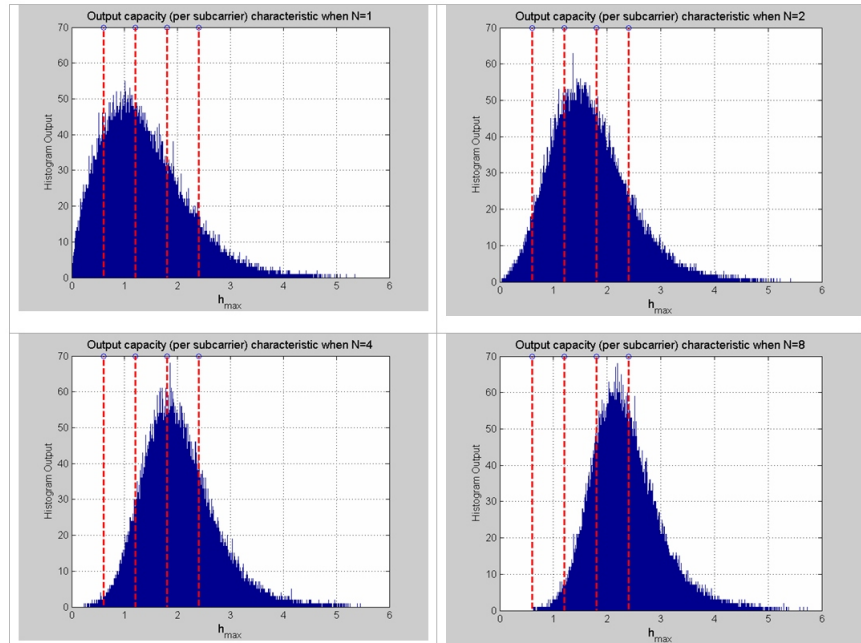


Figure 5.2: Output capacity (per subcarrier) characteristic w.r.t. N

#### 5.1.4 CALCULATION METHOD FOR THE PARAMETER “BALANCE RATIO”

In Section 5.1.3, it is explained that how the total incoming packet rate can be arranged according to desired load value:

$$\sum_{j=1}^N E\{a_j\} = L * K * \gamma_N. \quad (5.14)$$

Now it is time to explain that how the total incoming packet rate can be shared among users. In the literature, most of the studies such as [26], [6], [7], assume that the users are homogenous, i.e. they have statistically identical arrival processes. This means that all arrival rates,  $a_j$   $j \in \{1, 2, \dots, N\}$ , are equal to each other. However in real life, some of the users can be interested only in HTML pages (which corresponds to a relatively low arrival rate) and some of them can watch a video broadcast (which corresponds to a relatively high arrival rate) at the same time. Such scenerios cause “unbalance” situations among the arrival rate of the users. Because of this important and practical reason, in our thesis, we also simulate unbalanced situations in order to see the effect on the performances of subcarrier allocation algorithms.

**Definition 5.1.3** A “balance ratio” vector  $\mathbf{r} = \{r_1, r_2, \dots, r_N\}$  is a  $1 \times N$  vector such that each element  $r_j$  represents the ratio between the incoming packet rate of user  $j$  and the total incoming packet rate of the system.

$$r_j = \frac{E\{a_j\}}{\sum_{x=1}^N E\{a_x\}}, \forall j \in \{1, 2, \dots, N\}. \quad (5.15)$$

Note that the sum of all balance ratios is equal to 1:

$$\sum_{j=1}^N r_j = 1. \quad (5.16)$$

In order to create an unbalanced situation in our simulations, first we assign each member of the balance ratio vector  $\mathbf{r}$ , and then calculate the corresponding Poisson mean arrival rate per each user. Remember from Section 3.1.1 that

$$E\{a_j\} = \lambda_j * d \quad (5.17)$$

where  $d$  is the number of trials and  $\lambda_j$  is the probability that one packet arrives per each trial. So,  $\lambda_j$  can be chosen suitable for a desired unbalance situation, as follows:

$$E\{a_j\} = L * K * \gamma_N * r_j, \forall j \in \{1, 2, \dots, N\} \quad (5.18)$$

$$\lambda_j = \frac{L * K * \gamma_N * r_j}{d}, \forall j \in \{1, 2, \dots, N\} \quad (5.19)$$

## 5.2 SIMULATION RESULTS

Throughout this section, we investigate the effects of changing the number of users, the number of subcarriers, and the balance ratio on average throughput and average delay performances.

The common conditions valid for all simulations are given below as a list. The other parametric conditions are given as a table in their specific section.

- Simulation length = 10.000 timeslots
- Poisson distribution trial number,  $d = 1000$
- Rayleigh distribution variance,  $\sigma^2 = 1$
- All the graphs in Section 5.2.1 are plotted per each algorithm with respect to  $L=0.1$ ,  $L=0.3$ ,  $L=0.5$ ,  $L=0.6$  and  $L = L_i$  where  $L_i = 0.6 + (0.01 * i)$ ,  $i \in \{1, 2, \dots, 46\}$ .

### 5.2.1 THE EFFECT OF THE NUMBER OF USERS (N)

In many applications, such as IEEE.802.16e, the number of users is a dynamic parameter that can be changed anytime or any area. For example, the number of users can be changed with respect to hour (e.g. work hour) or date (e.g. holiday). Moreover, the population density of the region of operation also affects the number of users. So, a good algorithm should perform well even the number of users is changed dynamically. In this section, we investigate the performance of our algorithms with respect to  $N$ .

### 5.2.1.1 SIMULATION #1 (N=2)

The number of users, the number of subcarriers and the balance ratios for Simulation #1 are given at Table 5.2.

Table 5.2: Parameters for Simulation # 1

<b>N</b>	<b>K</b>	$r = \{r_1, r_2, \dots, r_N\}$
2	64	{0.5, 0.5}

Figure 5.3 shows the results of Simulation # 1. Note that, we zoom in on the important part of the second graph and re-plot the zoomed-in part as the third graph in Figure 5.3.

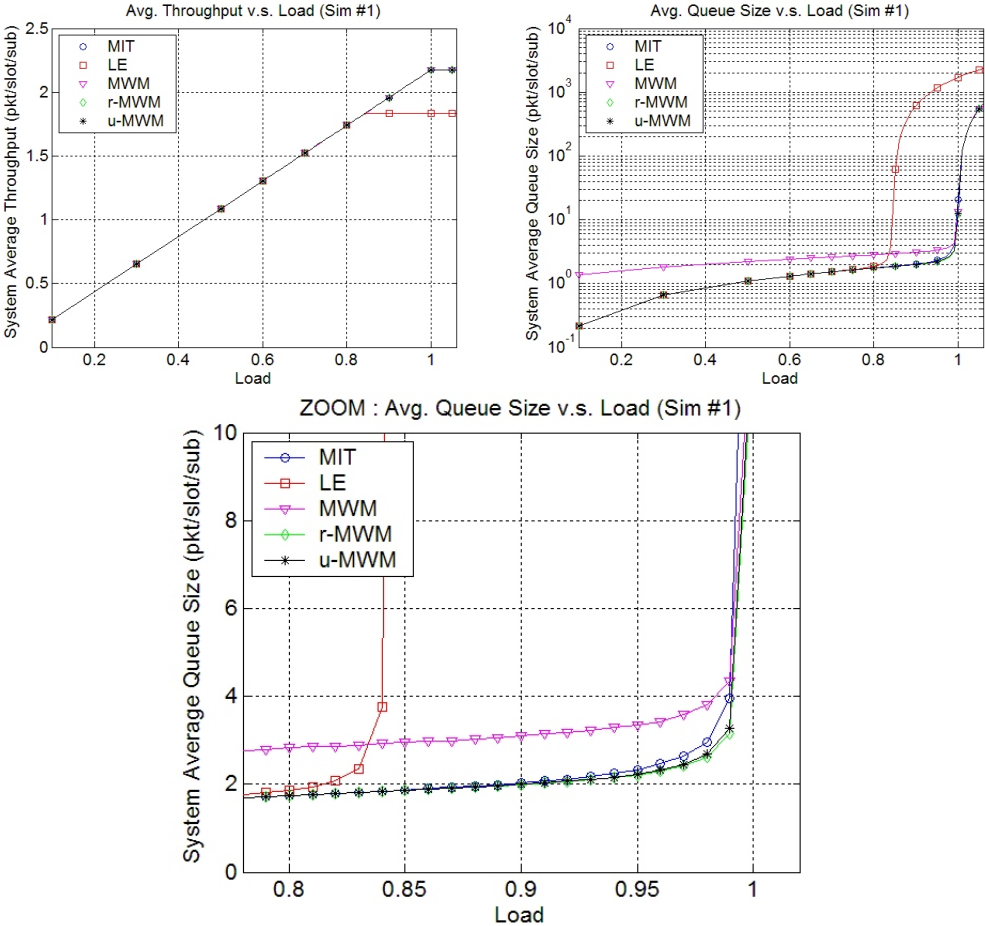


Figure 5.3: Simulation # 1 (N=2)

5.2.1.2 SIMULATION #2 (N=4)

The number of users, the number of subcarriers and the balance ratios for Simulation #2 are given at Table 5.3.

Table 5.3: Parameters for Simulation # 2

N	K	$r = \{r_1, r_2, \dots, r_N\}$
4	64	{0.25, 0.25, 0.25, 0.25}

Figure 5.4 shows the results of Simulation # 2.

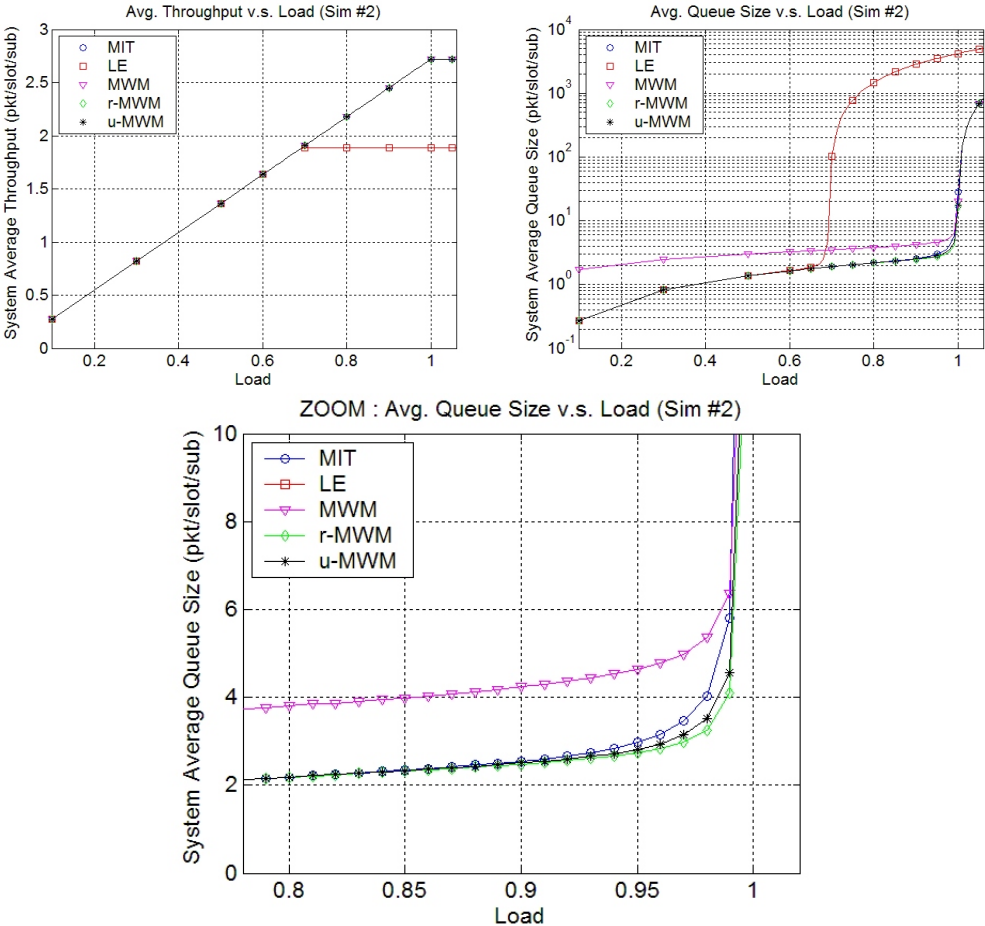


Figure 5.4: Simulation # 2 (N=4)

5.2.1.3 SIMULATION #3 (N=8)

The number of users, the number of subcarriers and the balance ratios for Simulation #3 are given at Table 5.4.

Table 5.4: Parameters for Simulation # 3

N	K	$r = \{r_1, r_2, \dots, r_N\}$
8	64	{0.125, 0.125, 0.125, 0.125, 0.125, 0.125, 0.125, 0.125}

Figure 5.5 shows the results of Simulation # 3.

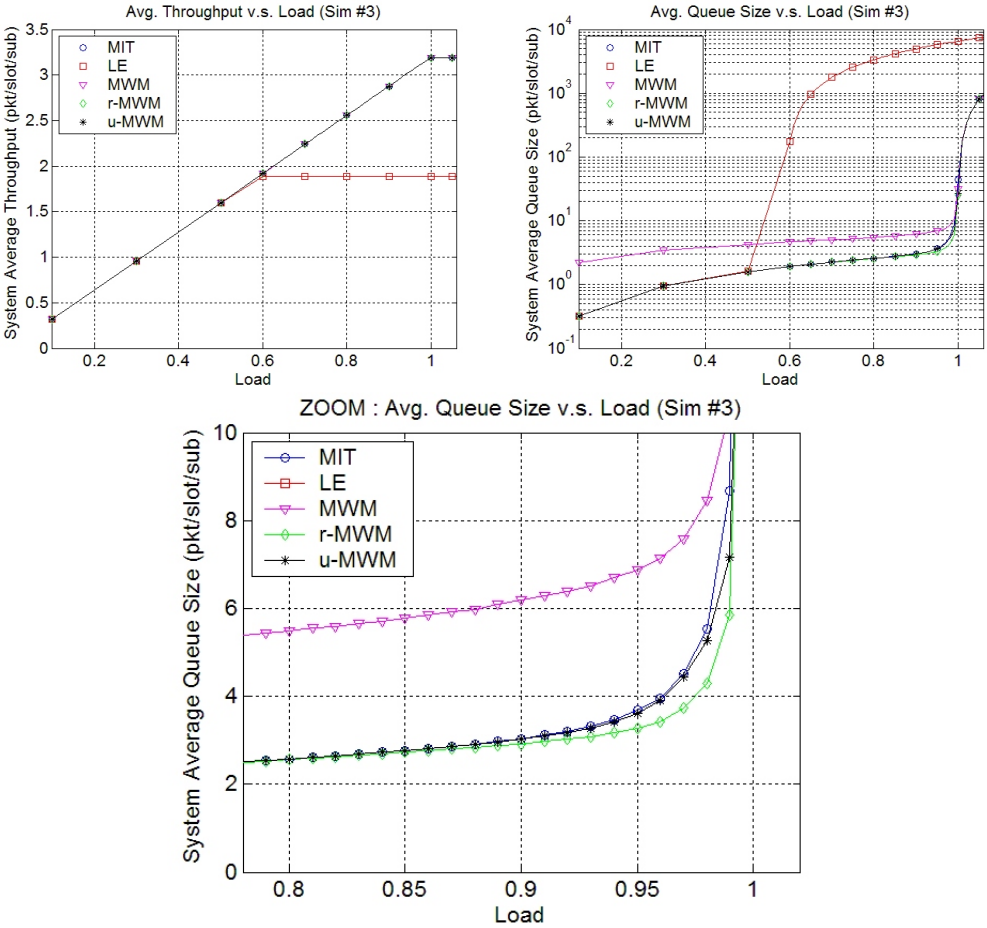


Figure 5.5: Simulation # 3 (N=8)

#### 5.2.1.4 SIMULATION RESULTS OF SIM. #1, #2 AND #3

After simulating the effect of changing the number of users on the performances of the algorithms, we can itemize the results obtained from these graphs.

1. All three simulations show that Maximum Weight Matching type algorithms (MWM, r-MWM, u-MWM) have the highest system average throughput in all cases. This result is an expected result because [5],[8],[30] show that MWM type algorithms are throughput optimal in long term case. Here, the interesting point is MIT algorithm also reaches the highest throughput values. This means that if the system is balanced i.e.  $r_a = r_b, \forall a, b \in \{1, 2, \dots, N\}$  and the channels are statistically identical to each user, then using only channel state information without using queue state information can be enough to reach the system average maximum throughput.
2. It is seen from the graphs that the LE throughput performance is the same as the other algorithms up to some load value, however after this load value the throughput of LE becomes saturated and even the incoming packet rate increases the throughput of LE can not increase. Moreover, when the number of users increases, the distance between the throughput saturated point of LE and other algorithms saturated points increases. This result can be explained with the help of “multiuser diversity” property. From Section 5.1.3, we know that if the number of users increases, the capacity per each subcarrier also increases. However, this multiuser diversity effect on throughput increment can be seen if a subcarrier allocation algorithm chooses the user with highest connectivity value among other users for a specific subcarrier. MIT, MWM, r-MWM and u-MWM algorithms take into account the connectivity values when deciding the allocation matrix,  $\mathbf{W}$ . So, as seen in the graphs, the maximum throughput (e.g. at load=1) of these algorithms increases with increasing the number of users. On the other hand, maximum throughput of LE does not increase with increasing the number of users. Roughly speaking, LE chooses the user with the highest queue sizes not the highest connectivity value. Just looking at the connectivity perspective, LE chooses  $c_{ij}$ 's randomly among users. As a result, multiuser diversity effect can not be seen with LE algorithm when there exists a balance in the system.
3. When looking at the average queue size v.s load graphs, in other words the delay performances of the algorithms, at lower load values all the algorithms except MWM has

nearly the same delay performance. But LE's queue size blows up earlier than the other algorithms. Note that the load value which the blowing up event occurs corresponds to the same load value where the throughput saturation point exists.

4. MWM has a higher average queue size but it's blowing up point is the same as the other algorithms except LE.
5. The remaining three algorithms MIT, r-MWM and u-MWM has nearly the same delay performances when there exists low to moderate incoming packet traffic regime (i.e. load  $\approx 0.9$ ). On the other hand, in heavy loaded case (i.e. load  $\approx 0.9$ ), the differences of the delay performances can be seen among three users. r-MWM has the lowest average queue size, second is the u-MWM and the third one is MIT. Let us remember that r-MWM has a higher calculation complexity than u-MWM and MIT algorithms.

### **5.2.2 THE EFFECT OF THE NUMBER OF SUBCARRIERS (K)**

The concept of "scalable subcarrier number" was introduced to the IEEE 802.16 Wireless-MAN Orthogonal Frequency Division Multiplexing Access (OFDMA) mode by the 802.16 Task Force Group e (TGe). A scalable physical layer in IEEE.802.16e enables standard-based solutions to deliver optimum performance in channel bandwidths ranging from 1.25 MHz to 20 MHz with fixed subcarrier spacing for both fixed and portable/mobile usage models, while keeping the product cost low. The architecture is based on a scalable subchannelization structure with variable Fast Fourier Transform (FFT) sizes according to the channel bandwidth ([32]).SOFDMA is a variant of OFDMA that allows for a variable number of subcarriers, based on the available bandwidth, without affecting the subcarrier spacing and other values that affect the higher-layer processing ([31]).

Table 2.4 depicts the scalability parameters for the SOFDMA modulation scheme employed by the IEEE 802.16e standard [33].

As explained above, the number of the subcarriers can also be a parameter for OFDMA systems. So, we also simulate the changing of the subcarrier number and investigate whether it has an effect on the system average throughput or delay.

### 5.2.2.1 SIMULATION #4 (K=8)

The number of users, the number of subcarriers and the balance ratios for Simulation #4 are given at Table 5.5.

Table 5.5: Parameters for Simulation # 4

<b>N</b>	<b>K</b>	$r = \{r_1, r_2, \dots, r_N\}$
4	8	{0.25, 0.25, 0.25, 0.25}

Figure 5.6 shows the results of Simulation # 4.

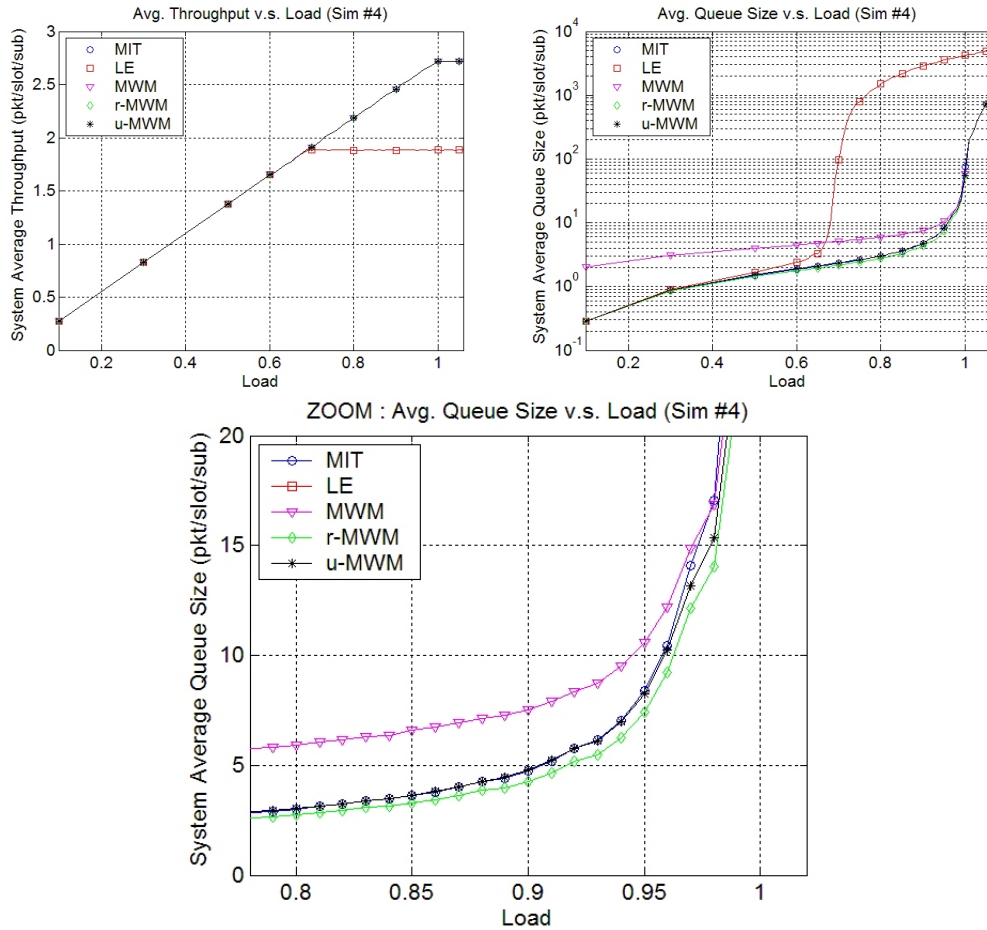


Figure 5.6: Simulation # 4 (K=8)

### 5.2.2.2 SIMULATION #5 (K=16)

The number of users, the number of subcarriers and the balance ratios for Simulation #5 are given at Table 5.6.

Table 5.6: Parameters for Simulation # 5

$N$	$K$	$r = \{r_1, r_2, \dots, r_N\}$
4	16	{0.25, 0.25, 0.25, 0.25}

Figure 5.3 shows the results of Simulation # 5.

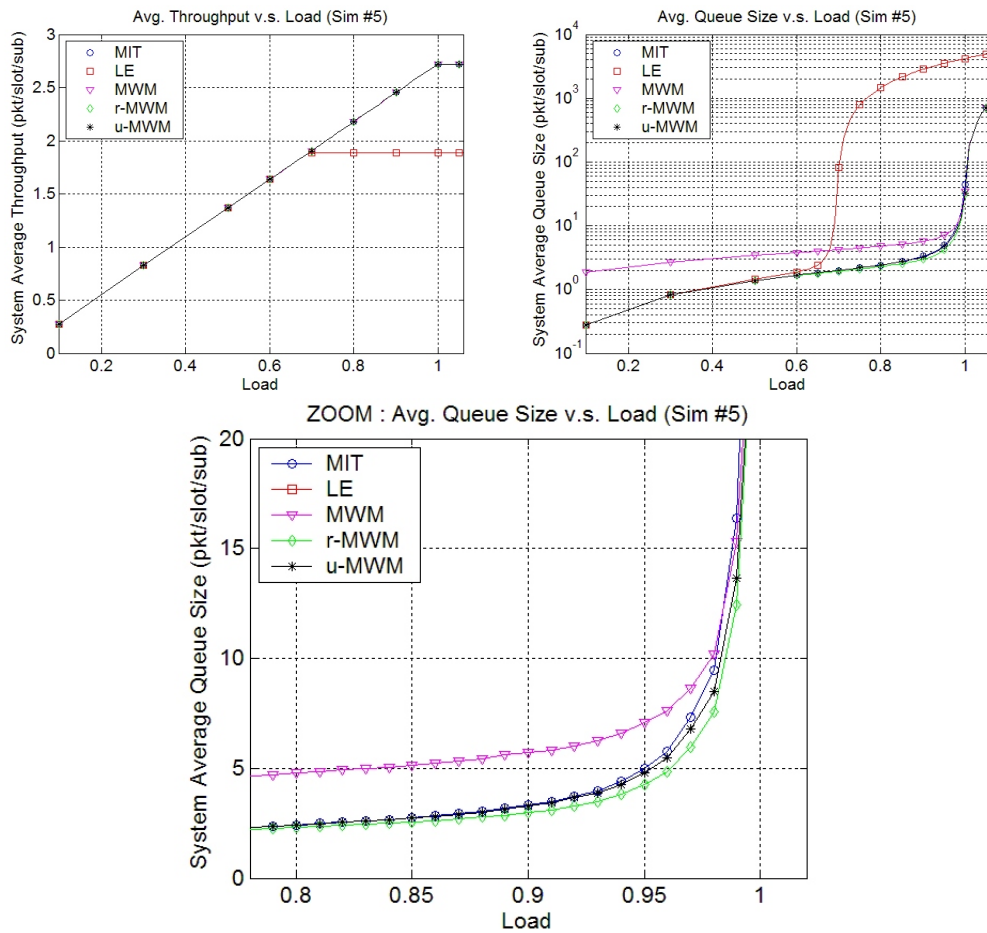


Figure 5.7: Simulation # 5 (K=16)

5.2.2.3 SIMULATION #6 (K=32)

The number of users, the number of subcarriers and the balance ratios for Simulation #6 are given at Table 5.7.

Table 5.7: Parameters for Simulation # 6

N	K	$r = \{r_1, r_2, \dots, r_N\}$
4	32	{0.25, 0.25, 0.25, 0.25}

Figure 5.3 shows the results of Simulation # 6.

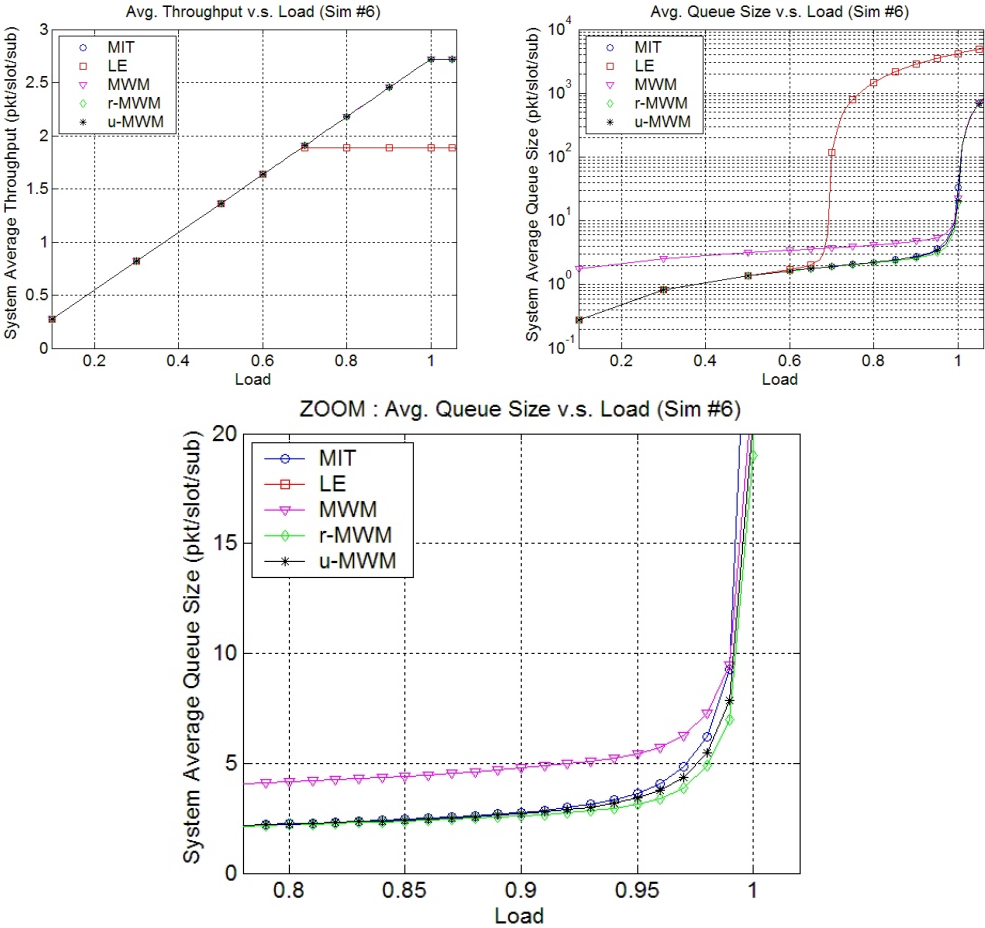


Figure 5.8: Simulation # 6 (K=32)

#### **5.2.2.4 SIMULATION RESULTS OF SIM. #4, #5 AND #6**

After simulating the effect of changing the number of subcarriers on the performances of the algorithms, we can itemize the results obtained from the graphs.

1. It can be seen from the graphs of simulation #4, #5 and #6, that changing the number of subcarriers does not have a significant effect on the throughput or delay performances of the algorithms with per subcarrier perspective. Throughout our study, we prefer to get the results “per subcarrier” unit (e.g. pkt/slot/subcarrier), and the simulation results support our preferences. In other words, the changing number of subcarriers effect can be discarded from the results in order to compare the algorithms and their performances with each other.
2. The only difference when increasing the subcarrier number is the slope of the average queue size blow up graph. If the number of subcarrier increases, the average queue size graph blows up more sharply.
3. The delay performance of the algorithms are still the same as explained in Section 5.2.1.4. Our proposed algorithm u-MWM performance is very close to r-MWM which has the highest complexity among the other algorithms.

#### **5.2.3 THE EFFECT OF THE BALANCE RATIO ( $r$ )**

Although most of the studies ([7], [9]) related with subcarrier allocation assume that the users are symmetric (i.e. they have statistically identical arrival processes), in real life each user’s data demands can be very different with each other. For this reason, the performances of the subcarrier allocation algorithms with varying balance ratio among users become an important issue. In this section, we investigate the average throughput and average delay performances of the algorithms with respect to balance and unbalance situations.

5.2.3.1 SIMULATION #7 ( $r=\{0.5, 0.5\}$ )

The number of users, the number of subcarriers and the balance ratios for Simulation #7 are given at Table 5.8.

Table 5.8: Parameters for Simulation # 7

$N$	$K$	$r = \{r_1, r_2, \dots, r_N\}$
2	32	$\{0.5, 0.5\}$

Figure 5.9 shows the results of Simulation # 7.

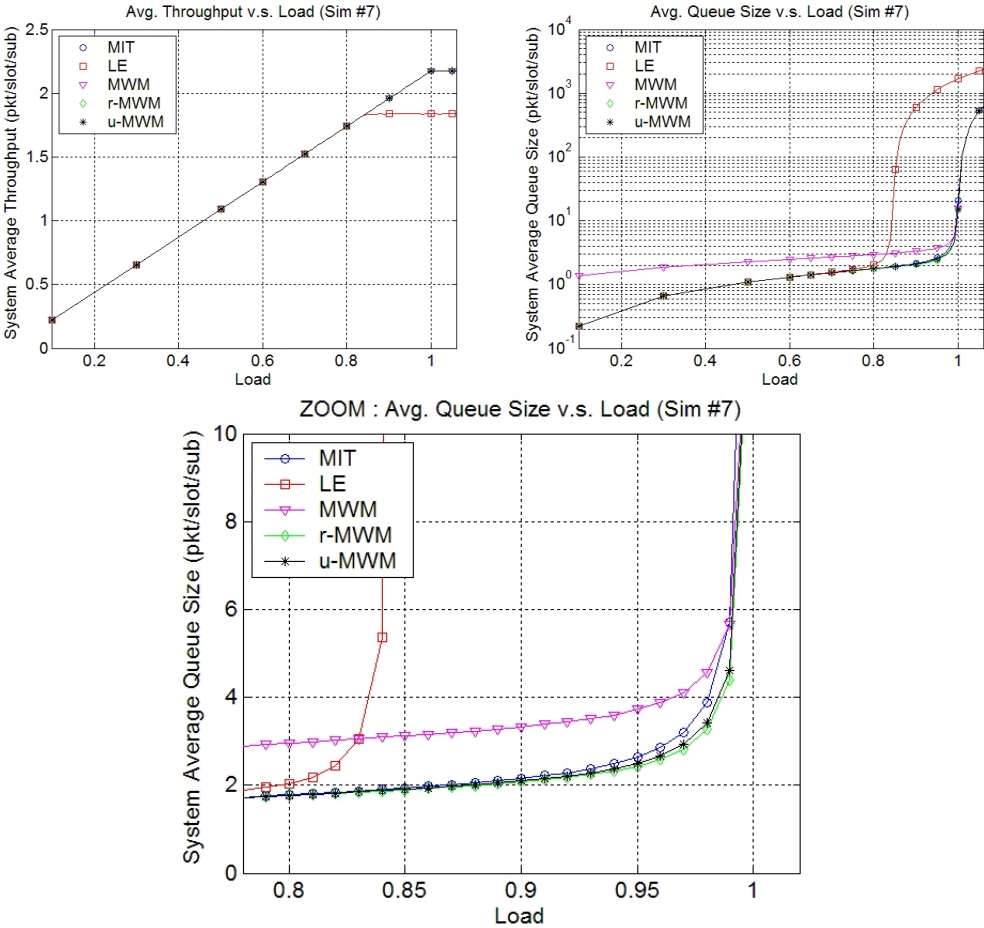


Figure 5.9: Simulation # 7 ( $r=\{0.5, 0.5\}$ )

5.2.3.2 SIMULATION #8 ( $r=\{0.7, 0.3\}$ )

The number of users, the number of subcarriers and the balance ratios for Simulation #8 are given at Table 5.9.

Table 5.9: Parameters for Simulation # 8

$N$	$K$	$r = \{r_1, r_2, \dots, r_N\}$
2	32	$\{0.7, 0.3\}$

Figure 5.10 shows the results of Simulation # 8.

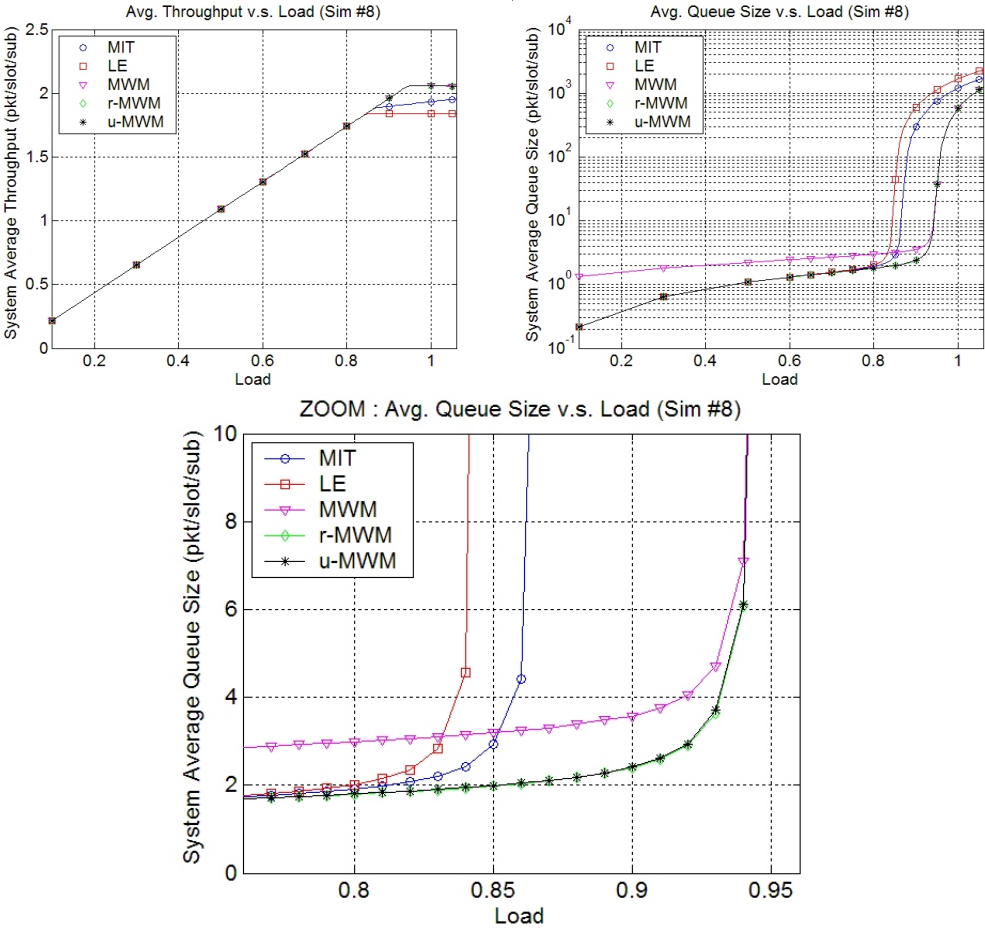


Figure 5.10: Simulation # 8 ( $r=\{0.7, 0.3\}$ )

5.2.3.3 SIMULATION #9 ( $r=\{0.9, 0.1\}$ )

The number of users, the number of subcarriers and the balance ratios for Simulation #9 are given at Table 5.10.

Table 5.10: Parameters for Simulation # 9

$N$	$K$	$r = \{r_1, r_2, \dots, r_N\}$
2	32	$\{0.9, 0.1\}$

Figure 5.11 shows the results of Simulation # 9.

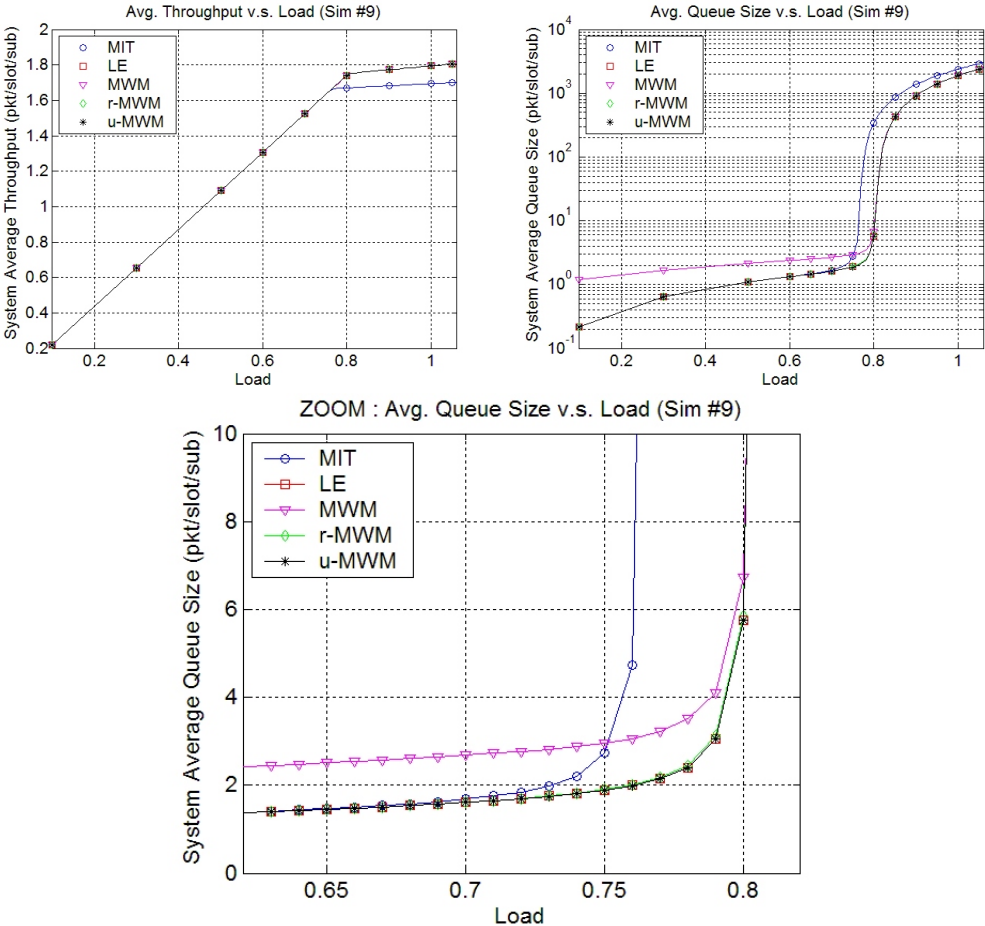


Figure 5.11: Simulation # 9 ( $r=\{0.9, 0.1\}$ )

#### 5.2.3.4 SIMULATION RESULTS OF SIM. #7, #8 AND #9

After simulating the effect of changing the balance ratio on the performances of the algorithms, we can itemize the results obtained from the graphs.

1. One of the most important result obtained from Simulation #7, #8 and #9 is the behaviour of MIT and LE algorithms with respect to different balance ratios. When the system is balanced, i.e.  $r_1 = r_2 = 0.5$ , the result of simulation #7 becomes very similar to the results given in Figure 5.3. On the other hand, if the system starts to be more unstable (e.g.  $r_1$  increases  $r_2$  decreases), then the throughput performance of MIT starts to decrease more rapidly relative to MWM, r-MWM and u-MWM. And after a specific balance ratio, MIT becomes the worst algorithm in terms of system average throughput among the other algorithms.
2. When the system's unbalanced characteristic increases, the throughput performance of MWM, r-MWM and u-MWM algorithms also decreases like MIT. This event again can be explained with the help of "multiuser diversity" term. Assume that  $r_1 \gg r_2$ . Then user-2 receives very small amount of packets. So the probability of the occurrence of an empty queue increases. If any user has an empty queue, it can not provide an alternative for selecting the highest connectivity value for the system, so it can not increase the multiuser diversity. Because of this, the throughput performance of the algorithms that benefits from the multiuser diversity starts to decrease when increasing the instability.
3. When highly unbalanced case, LE performs very well in terms of both average throughput and average delay criterias.
4. These simulations show us very clearly that there is a trade-off between MIT algorithm and LE algorithm. MIT algorithm aims to maximize the current time throughput. However, LE algorithm aims to maximize the future throughput by avoiding the idling of subcarriers caused by some empty queues. MIT algorithm works well when the queues are naturally balanced and there exists a small probability of occurring empty queues. When system unbalanced characteristic increases, then probability of occurring empty queues also increases and LE starts to perform well rather than MIT. MWM-type algorithms always perform well in terms of throughput, because they use both queue state information and channel state information. So in balanced case, channel state informa-

tion makes MWM-type algorithms perform well and in unbalanced case, queue state information makes them perform well.

5. In all different balance ratio cases, the delay performance of u-MWM is almost the same or exactly the same as the delay performance of r-MWM. This shows that, there is no need to use a high order complex algorithm to obtain a better average delay. u-MWM algorithm can also do this with low order complexity.

### 5.2.3.5 THE EFFECT OF ELEPHANT-MOUSE POPULATION

In Section 5.2.3, we have seen that the balance ratio has an important role on the performances of the subcarrier allocation algorithms. In that section (Sect.5.2.3), we prefer to simulate the case where there are 2 users ( $N=2$ ). This is the easiest way to understand the behaviour of the algorithms according to the changing balance ratios, because  $N=2$  case is a two dimensional problem and can be plot on a paper easily. For example, when the balance ratio of user-1 ( $r_1$ ) increases, the balance ratio of user-2 ( $r_2$ ) automatically decreases and so, we can easily say that the “unbalance” characteristic of the system increases. However, if the number of users is more than 2, identifying the unbalance characteristic of the system becomes not so easy.

After studying and simulating many cases, we have observed that even the number of users is greater than 2, it is still possible to understand the system “balance” characteristic which affects the performances of the algorithms.

In order to explain the multiuser case for  $N > 2$ , we use the definition of “elephant-mouse population”. We think that some of the members of the system (or of the population) can be identified as an elephant or a mouse. If the average incoming packet rate of user-a is much greater than the system average incoming packet rate per each user, then user-a can be called as an “elephant”. On the other hand, If the average incoming packet rate of user-b is much smaller than the system average incoming packet rate per each user, then user-b can be called as a “mouse”.

First, let’s look at the effect of one elephant in an  $N$ -member population. Table 5.11 shows the parameters used in Simulation #10 which simulates that one user in the system gets 75% of incoming packets of total received packets and other 7 users get 3.57% each.

Table 5.11: Parameters for Simulation # 10

<b>N</b>	<b>K</b>	$r = \{r_1, r_2, \dots, r_N\}$
8	32	{0.75, 0.0357, 0.0357, 0.0357, 0.0357, 0.0357, 0.0357, 0.0357, 0.0357}

Figure 5.12 shows the results of Simulation #10.

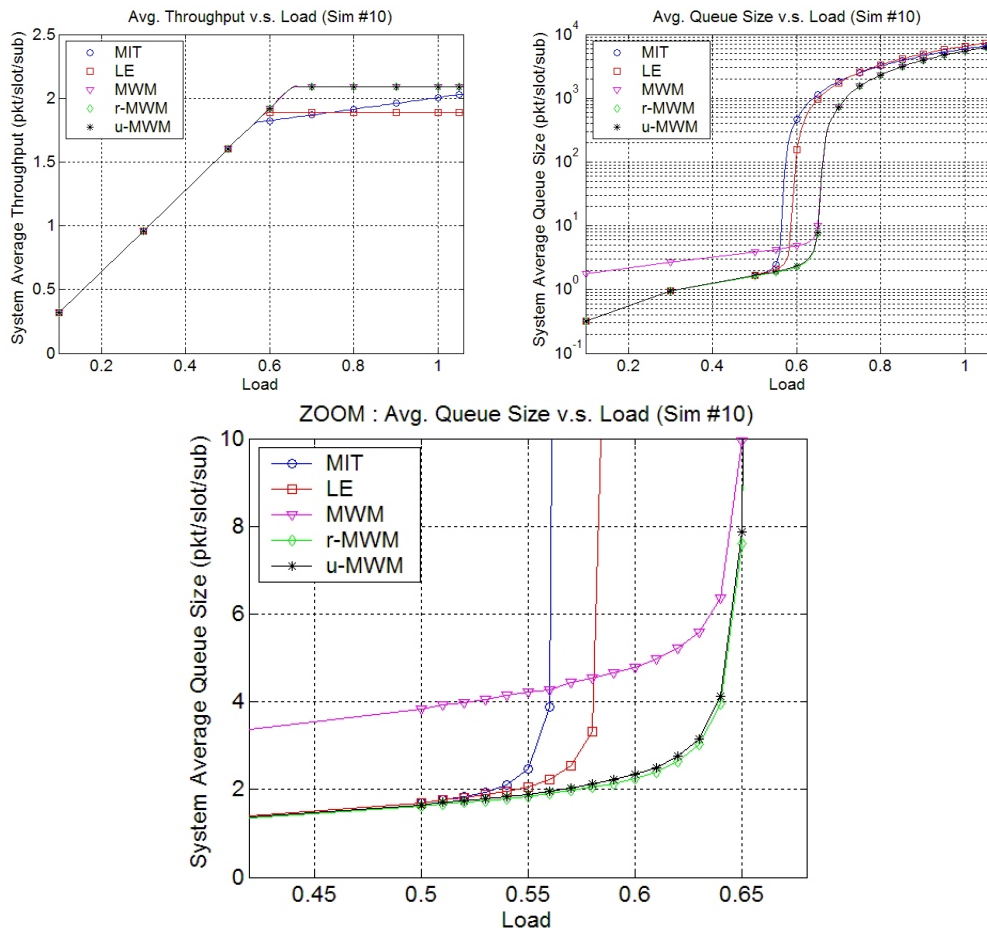


Figure 5.12: Simulation # 10 ( $r=\{0.75, 0.0357, \dots, 0.0357\}$ )

As seen in Figure 5.12, we obtain very similar results given in Figure 5.10.

Now, let's look at the effect of one mouse in an N-member population. Table 5.12 shows the parameters used in Simulation #11 which simulates that one user in the system gets only 2% of incoming packet of total received packets and other 7 users get 14% each.

Figure 5.13 shows the results of Simulation #11.

Table 5.12: Parameters for Simulation # 11

<b>N</b>	<b>K</b>	$r = \{r_1, r_2, \dots, r_N\}$
8	32	{0.02, 0.14, 0.14, 0.14, 0.14, 0.14, 0.14, 0.14, 0.14}

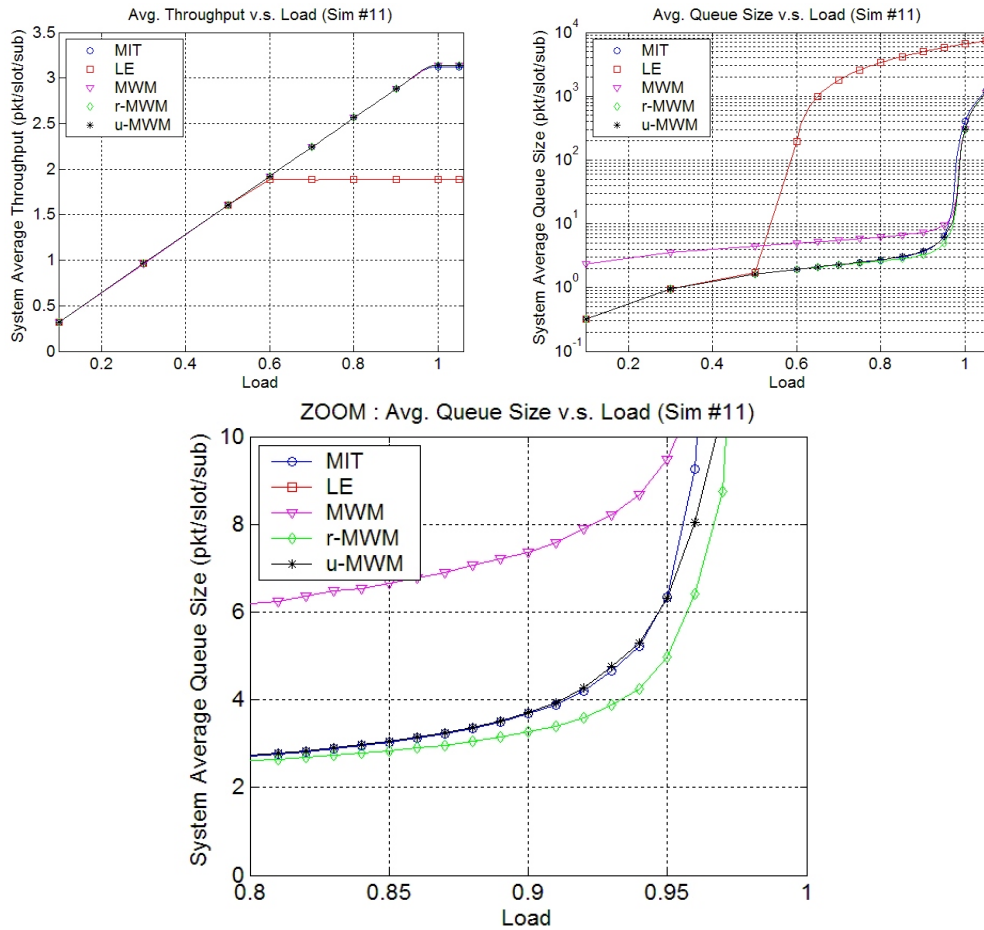


Figure 5.13: Simulation # 10 ( $r=\{0.02, 0.14, \dots, 0.14\}$ )

This time, we obtain the results very similar to graphs given in Figure 5.9. This is very interesting, because Figure 5.9 represents a “balanced” system case. This issue can be explained as follows: although one mouse creates an unbalance situation in N-member population, (N-1) members, the dominant part of the system, are still balanced among each others. Because of this reason, we obtain again a balanced-like system results.

Finally, it is clearly seen from Simulation #10 and #11 that “elephants” have more and dominant effects on increasing the system unbalance characteristic than the “mouses”.

#### 5.2.4 OBTAINING THE STABILITY REGION WITH A SIMULATION-BASED TECHNIQUE

In real life, because of the impossibility of having infinite queue lengths, the “stability” becomes one of the most important issues for systems which have queues. In general definition, the system is called “stable” if the queue length process reaches a steady state and does not blow to infinity. In the literature, there are many stability definitions ([30], [5], [8]) for network systems. Most of them has the same idea which is that when time goes to infinity, the queue length of the stable system should not go to infinity. As an example, [30] defines the stability as given in Definition 5.2.1.

**Definition 5.2.1** *Let  $A_j(n)$  denote the number of packets that have arrived at queue- $j$  up to timeslot  $n$ . Assume that  $A_j(n) = 0$  and the arrival process  $\{A_j(\cdot), j = 1, 2, \dots, N\}$  satisfy a strong law of large numbers (SLLN) : with probability one,*

$$\lim_{n \rightarrow \infty} \frac{A_j(n)}{n} = \lambda_j, j \in \{1, 2, \dots, N\} \quad (5.20)$$

where  $\lambda_j$  is called the arrival rate of queue- $j$ . Now, let  $D_j(n)$  be the number of departures from queue- $j$  up to time slot  $n$  and  $D_j(0) = 0$ . The system is said to be **rate stable** if, with probability one,

$$\lim_{n \rightarrow \infty} \frac{D_j(n)}{n} = \lambda_j, j \in \{1, 2, \dots, N\} \quad (5.21)$$

for any arrival process satisfying Eqn.5.20.

Each subcarrier allocation algorithms has its own stability regions and these regions give us a valuable information about the algorithm’s throughput performance. [5] shows that the stability region of a throughput optimal policy covers the whole stability regions of any policies. So roughly speaking, the largest the stability region the better the policy is, in terms of throughput.

Both the simulation and analysis approaches are useful for determining network stability. The analytical approach considers a class of network models, answering with certainty whether the class is stable, or providing no answer because the network class is intractable. The simulation approach considers a particular network, always answering but with some uncertainty. Compared to probability analysis, using simulation to check stability has the advantages that

it applies to any queueing network, it always provides an answer and the practitioner needs only to provide a simulation code.

When comparing the stability regions of our subcarrier allocation algorithms, we prefer to choose the simulation approach. In the literature, there are some studies such as [34], [35], [36] which are interested in identifying the network system whether it is stable or not via some simulations. With the help of these studies, we develop our own method which is simpler and more applicable to our system model described in Section 3.1. Before explaining our own method, let us give some information about obtaining the stability boundary on the graph. We give an example with  $N=2$  which is easy to visualize in 2-D plot.

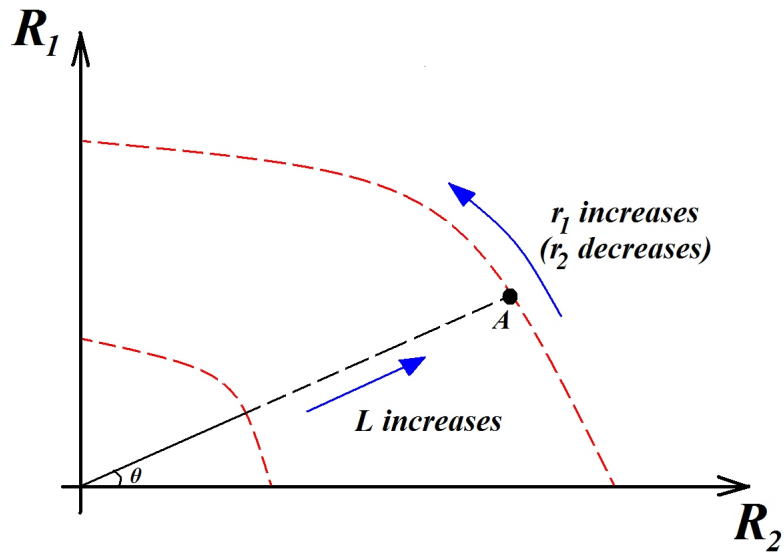


Figure 5.14: The effect of load and balance ratio on throughput region

As seen in Figure 5.14, the throughput of user-1,  $R_1$ , is located on the y-axis and the throughput of user-2,  $R_2$ , is located on the x-axis. The point A is the cross section point of  $R_1$  and  $R_2$ . In order to obtain the stability boundary, starting from the origin, all  $(R_1, R_2)$  couples should be observed and decided whether the system is stable at that point A corresponding to  $(R_1, R_2)$ . In our model, this tracking on the plane can be done by changing the load (L) values and balance ratios ( $\mathbf{r}=\{r_1, r_2\}$ ). Generally (but not necessarily all the time), increasing the load value increases the distance between the origin and the point A. Moreover, increasing the balance ratio of user-1,  $r_1$ , rotates the position of point A to the left, and increasing  $r_2$  rotates the position of point A to the right. With the help of our simulations, we have seen that this

behaviour is valid most of the time but can be changed unpredictably beyond the stable region (unstable region).

In order to obtain different  $(R_1, R_2)$  couples, first we fix the balance ratio and then start to increase the load values. After reaching the end of the stable region (reaching the stability boundary), then we change balance ratio and start to increase the load value again starting from the origin. If the discretization of load and balance ratio values are chosen properly, it is possible to obtain a very good approximation of the stability region boundary with this method. Here, the most critical point is deciding whether the point A corresponding to  $(R_1, R_2)$  is in the stable region or outside the stable region. In Section 5.2.4.1, we explain our proposal method for deciding the stability of point A.

#### 5.2.4.1 SIMULATION BASED STABILITY CHECKING METHOD

In this section, we explain our proposed simulation based stability checking method step by step.

Step 1: Define the simulation length,  $S$  in slot time unit. The longer the simulation length, the more accurate the result is. In our simulations,  $S$  is equal to 10.000 slots.

Step 2: Define the batch number,  $B$ . This number defines the number of subgroups of the simulation slots which are used for obtaining some statistical results. In our simulations,

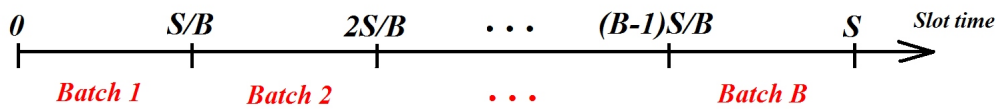


Figure 5.15: Batching the slot time

the batch number  $B$  is set to 20.

Step 3: Run the simulation with the investigated algorithm and investigated simulation parameters  $(N, K, \mathbf{r})$  up to simulation slot time  $S$ . At each slot time, log the each user' queue lengths.  $(\mathbf{b}(\mathbf{n}) = (b_1(n), b_2(n), \dots, b_N(n)), n \in \{1, 2, \dots, S\})$

Step 4: After the end of the simulation, calculate the average number of queue lengths for

each user per each batch in pkt/subcarrier unit.

$$b_{j,x} = \frac{\sum_{n=(x-1)\frac{S}{B}+1}^{x\frac{S}{B}} b_j(n)}{\frac{S}{B}K}, j \in \{1, 2, \dots, N\}, x \in \{1, 2, \dots, B\} \quad (5.22)$$

Step 5: Calculate the overall average number of queue lengths per subcarrier for each user.

The first batch values are not included to calculations because reaching the steady state from transient state occurs in Batch 1 and the transient state information can fake the result.

$$b_{j,avg} = \frac{\sum_{x=2}^B b_{j,x}}{(B-1)}, j \in \{1, 2, \dots, N\} \quad (5.23)$$

Step 6: Per each user, find how many  $b_{j,x}$  ( $x \in \{2, 3, \dots, B\}$ ) values are outside the  $(b_{j,avg} - c_{cap}/2, b_{j,avg} + c_{cap}/2)$  region where  $c_{cap}$  represents the max. connectivity value. In our model, the maximum connectivity value is 4 ( $c_{cap} = 4$ ).

Step 7: For any user, if the number of  $b_{j,x}$  ( $x \in \{2, 3, \dots, B\}$ ) outside the region given in Step-6 is equal to or greater than  $B/2$ , then the system is called “unstable”, otherwise the system is called “stable”.

The main idea of this method is as follows: considering the batch values, if any users’ queue length characteristic is outside the region defined in Step-6 more than 50% in time, then the system is assumed to be unstable. As an example, Figure 5.16 shows one of the instability case.

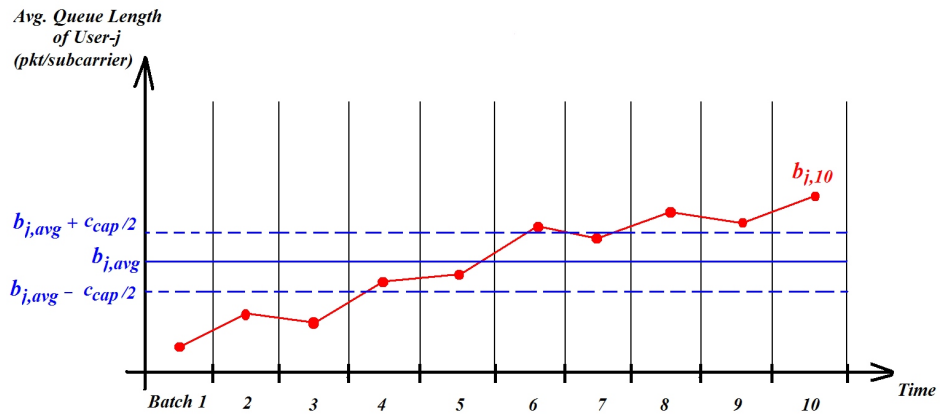


Figure 5.16: Examples of the instability

Our heuristic method for checking the stability may not be an optimal method, but we have seen from the simulation results that the method works very well with our system model. Figure 5.17 shows the stability regions of our interested algorithms when  $N=2$  and  $K=32$ . This result can be compared with the Simulation #7, #8 and #9 results and can be seen that the stability boundary points in Figure 5.17, completely matches with the queue blow up points showing in Simulation #7, #8 and #9.

**5.2.4.2 COMPARISONS OF THE STABILITY REGIONS OF THE ALGORITHMS**

In this section, with the help of the method explained in Section 5.2.4 and 5.2.4.1, we obtain the stability regions of the subcarrier allocation algorithms. We simulate for  $N=2$  users and  $K=32$  subcarriers case. Balance ratio is parametric and takes the values of  $r=\{0.01,0.99\}$ ,  $\{0.1,0.9\}$ ,  $\{0.2,0.8\}$ , ...,  $\{0.8,0.9\}$ ,  $\{0.9,0.1\}$ ,  $\{0.99,0.01\}$ .

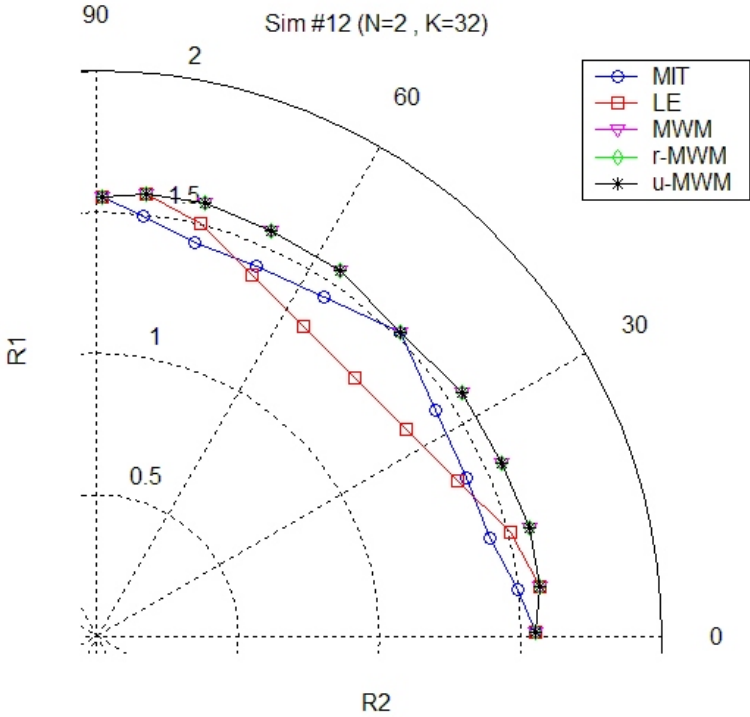


Figure 5.17: Simulation # 12 (N=2, K=32)

As seen in Figure 5.17, all three MWM algorithms have the largest stability region. This is an expected result because in [5],[8],[30] it is proved that the MWM type algorithms are

throughput optimal and have the largest stability regions. The interesting results in the graph are the stability characteristics of MIT and LE algorithms. When there exists a balance i.e.  $r=\{0.5,0.5\}$ , MIT which uses channel state information performs very well. On the other hand, LE which uses queue state information has a poor performance in terms of throughput in balanced case. However, when the system's unbalanced characteristic increases, LE starts to become better than MIT algorithm.

## CHAPTER 6

### CONCLUSION AND FUTURE WORK

In this thesis, we have considered the problem of subcarrier allocation in OFDMA systems. We have compared five subcarrier allocation algorithms in terms of the system average throughput and the system average delay criteria. Each algorithm was selected carefully so that each one differentiate with others with its different aspect of allocating subcarriers. For example, the MIT algorithm uses channel state information, on the other hand the LE algorithm uses queue state information for deciding the subcarrier allocation. The MWM algorithm uses both channel and queue state information, but it is not interested in minimizing the delay. r-MWM algorithm considers maximizing the throughput and minimizing the delay with the help of channel and queue state information, however this time it increases the calculation complexity compared to other algorithms. Finally, the fifth algorithm, u-MWM, has been proposed by us and we have argued that this algorithm considers both throughput and delay issues using channel and queue state information and also provides a lower complexity order than r-MWM algorithm.

We have simulated the delay and throughput performances of the allocation algorithms with respect to the number of users, the number of subcarriers, the load, and the balance ratio parameters. With the help of our simulations, we have observed many results which help us understand the behavior of the algorithms under different conditions.

We have seen from the simulations that increasing the number of subcarriers does not have a significant effect on the throughput or delay performances of the systems. So, obtaining the throughput and queue sizes in per subcarrier unit (e.g. packet/slot/subcarrier) becomes reasonable in order to eliminate one parameter for comparing the other parameters.

We have also observed that increasing the number of users improves the throughput perfor-

manances of MIT, MWM, r-MWM and u-MWM. On the other hand, the throughput performance of LE is not affected by the number of users. In the thesis, this phenomenon has been explained by using “multiuser diversity” term. Roughly speaking, the more users a base station services, the higher the probability of finding a higher connectivity value for each subcarrier. This effect increases the capacity of each subcarrier and is called multiuser diversity. Note that LE is the only algorithm among the others which does not consider the channel state information and thus, it is the only algorithm which can not benefit from multiuser diversity.

In our thesis, some interesting observations has been made when varying the balance ratio values. For example, when the system is balanced, the throughput performance of the MIT algorithm reaches the throughput performance of MWM-type algorithm which are MWM, r-MWMW and u-MWM. We know from [8] that MWM-type algorithms are throughput optimal, so the MIT algorithm also achieves the system average throughput limits with only using the channel state information when the channels are statistically identical among users. When changing the balance ratio in order to increase the “unbalanced” characteristic of the system, we have seen that the throughput performance of MIT decreases more rapidly than MWM-type algorithms, while the throughput performance of LE almost remains constant. Moreover, beyond some balance ratio, LE starts to perform better than MIT in terms of average throughput. Finally all these findings show us that in balanced case the channel state information is more critical, on the other hand in unbalanced case the queue state information and balancing the queues become more critical.

When considering the delay issues, simulations show us that r-MWM has the minimum system average delay under all simulated scenarios. However the interesting point is that, our proposed algorithm u-MWM also reaches almost or exactly the same delay performance of r-MWM with a lower computational complexity. So, u-MWM algorithm becomes a unique algorithm which meets the three criteria (maximum throughput, minimum delay, low complexity) at the same time.

Simulation-based checking the stability of a system is one of the most important parts in our thesis. Rather than using analysis methods, we have proposed our simulation based method which can decide whether the system is stable or not at that scenario. By using this method, we have also obtained the stability regions of subcarrier allocation algorithms for  $N=2$  users. Note that, this method can also be directly applied for  $N>2$ .

Finally, we note that investigating the subcarrier allocation algorithms in terms of fairness perspective is an interesting problem for further investigations. Moreover, the effect of the statistically non-identical channel connectivities on system throughput and delay performances can be a valuable study topic for future research.

## REFERENCES

- [1] M. Ergen, S. Coleri, P. Varaiya, "QoS aware adaptive resource allocation techniques for fair scheduling in OFDMA based broadband wireless access systems", *IEEE Trans. on Broadcasting*, vol.49, no.4, Dec. 2003.
- [2] J.Jang, K.B.Lee, Y.H.Lee, "Transmit power and bit allocations for OFDM systems in a fading channel", *Proc. IEEE GLOBECOM 2003*.
- [3] W. Rhee, J.M.Cioffi, "Increase in capacity of multiuser OFDM system using dynamic subchannel allocation", *Proc. of Vehicular Tech Conf. (VTC) 2000*, vol.2, pp.1085-1089, May 2000.
- [4] S. Pfletschinger, G. Munz, J. Speidel, "An efficient waterfilling algorithm for multiple access OFDM", *IEEE GLOBECOM 2002*, Nov. 2002.
- [5] L. Tassiulas, A. Ephremides, "Stability properties of constrained queueing systems and scheduling policies for maximum throughput in multihop radio networks", *IEEE Trans. on Automatic Control*, vol.37, no.12, Dec. 1992.
- [6] S. Kittipiyakul, T. Javidi, "A fresh look at optimal subcarrier allocation in OFDMA systems", *Proc. IEEE Conference on Decision and Control*, Dec. 2004.
- [7] L. Tassiulas, A. Ephremides, "Dynamic server allocation to parallel queues with randomly varying connectivity", *IEEE Trans. on Info. Theory*, vol.39, no.2, March 1993.
- [8] T. Javidi, "Rate stable resource allocation in OFDM systems: from waterfilling to queue-balancing", *Proc. Allerton Conference on Communication, Control and Computing*, 2004.
- [9] S. Kittipiyakul, T. Javidi, "Resource Allocation in OFDMA with Time-Varying Channel and Bursty Arrivals", *IEEE Communications Letter*, vol.11, no.9, Sept. 2007.
- [10] R. Prasad, "OFDM For Wireless Communications Systems", Artech House, 2004.
- [11] S.B.Weinstein, P.M.Ebert, "Data Transmission by Frequency Division Multiplexing Using the Discrete Fourier Transform", *IEEE Trans. Communications*, vol.19, pp.628-634, Oct. 1971.
- [12] B.Canpolat, "Performance Analysis of Adaptive Loading OFDM under Rayleigh Fading with Diversity Combining", *Ph.D. Thesis, METU*, Sept. 2001.
- [13] R.D.Yates, D.J.Goodman, "Probability and Stochastic Processes", John Wiley & Sons, pp. 210-215, 1999.
- [14] K.S.Trivedi, "Probability and Statistics with Reliability, Queuing and Computer Science Applications", John Wiley & Sons, pp. 304-314, 2002.

- [15] F. Beichelt, "Stochastic Process in Science, Engineering and Finance", Chapman & Hall/CRC, pp. 113-126, 2006.
- [16] M. Pätzold, "Mobile Fading Channels", John Wiley & Sons, pp.33-53, 2002.
- [17] W. R. Young, "Comparison of mobile radio transmission at 150, 450, 900 and 3700 MHz", Bell Syst. Tech. J., vol. 31, pp. 1068-1085, Nov. 1952.
- [18] H. W. Nylund, "Characteristics of small-area signal fading on mobile circuits in the 150 MHz band", IEEE Trans. Veh. Technology, vol. 17, pp. 24-30, Oct. 1968.
- [19] Y. Okumura, E. Ohmori, T. Kawano, K. Fukuda "Field strength and its variability in VHF and UHF land mobile radio services", Rev. Elec. Comm. Lab., vol. 16, pp. 825-873, Sep./Oct. 1968.
- [20] "Understanding the Radio Technologies of WiMAX and Their Effect on Network Deployment Optimization", Alvarion white paper, 2006.
- [21] S. Hara, R. Prasad, "Multicarrier Techniques for 4G Mobile Communications", Artech House, pp.14-18, 2003.
- [22] A. Goldsmith, "Wireless Communications", Cambridge Press, pp.70-79, pp.283-320, 2005.
- [23] J.F. Hayes, "Adaptive feedback communications", IEEE Trans. Commun. Tech., pp.29-34, February 1968.
- [24] J.K. Cavers, "Variable-rate transmission for Rayleigh fading channels", IEEE Trans. Commun. pp.15-22, February 1972.
- [25] A. Czylik, "Adaptive OFDM for wideband radio channels", in Proc. GLOBECOM '96, vol. 1, pp.713-718, 1996.
- [26] S. Kittipiyakul, T. Javidi, "Delay-optimal server allocation in multi-queue multi-server systems with time-varying connectivities", submitted to IEEE Trans. on Info Theory, May, 2007.
- [27] G. Li, H. Liu, "Dynamic resource allocation with finite buffer constraint in broadband OFDMA networks", IEEE Wireless Comm. and Networking, vol. 2, pp. 1037-1042, March 2003.
- [28] D.P. Bertsekas, R. Gallager, "Data Networks", New Jersey: Prentice-Hall Inc., 1992.
- [29] C. Yih, E. Geraniotis, "Adaptive modulation, power allocation and control for OFDM wireless networks", Proc. IEEE Int. Symp. on Personal, Indoor, Mob. Radio Commun., vol.2, pp.813-819, 2000.
- [30] J.G. Dai, B. Prabhakar, "The throughput of data switches with and without speedup", Proc. of IEEE INFOCOM pp.556-564, 2000.
- [31] U.S. Jha, R. Prasad, "OFDM, towards fixed and mobile broadband wireless access", Artech House, 2007.
- [32] H. Yaghoobi, "Scalable OFDMA Physical Layer in IEEE 802.16 WirelessMAN", Intel Technology Journal, vol.8, issue-3, August 2004.

- [33] IEEE 802.16e-2005, “IEEE Standard for Local and Metropolitan Area Networks. Part 16: Air Interface for Fixed and Mobile Broadband Wireless Access Systems, Amendment 2:Physical and Medium Access Control Layers for Combined Fixed and Mobile Operation in Licensed Bands and Corrigendum 1”, Feb. 2006.
- [34] J.R. Wieland, R.Pasupathy, B.W. Schmeiser, “Queueing-network stability: simulation-based checking”, Proc. of the Winter Simulation Conference, 2003.
- [35] J.Banks, J.G.Dai, “Simulation studies of multiclass queueing networks”, IEEE Transaction 29, pp.213-219, 1997.
- [36] J.G.Dai, S.P. Meyn, “Stability and convergence of moments for multiclass queueing networks via fluid limit models”, IEEE Transactions on Automatic Control, vol.40, no.11, Nov. 1995.

## APPENDIX A

### LITTLE'S THEOREM

**Theorem A.0.2** *The long-term average number of packets  $\bar{P}$  in a stable system, is equal to the long-term average arrival rate  $\lambda$  multiplied by the long-term average time that a packet spends in the system  $\bar{T}$ :*

$$\bar{P} = \lambda \bar{T} \quad (\text{A.1})$$

**Proof.** Define the following:

- $\alpha(t)$  = number of packet arrivals in the interval of  $(0, t)$
- $\delta(t)$  = number of packet departures in the interval of  $(0, t)$
- $P(t)$  = number of packets in the system at time  $t$  ( $P(t) = \alpha(t) - \delta(t)$ )
- $\gamma(t)$  = accumulated packets - timeslots in the interval of  $(0, t)$

These functions are graphically shown in Figure A.1.

The colored area in Figure A.1 between the arrival and departure curves is  $\gamma(t)$ .

$\lambda_t$  = arrival rate over  $(0,t)$ ,

$$\lambda_t = \frac{\alpha(t)}{t} \quad (\text{A.2})$$

$\bar{P}_t$  = average number of packets during the interval  $(0,t)$ ,

$$\bar{P}_t = \frac{\gamma(t)}{t} \quad (\text{A.3})$$

$\bar{T}_t$  = average time that a packet spends in the system in  $(0,t)$ ,

$$\bar{T}_t = \frac{\gamma(t)}{\alpha(t)} \quad (\text{A.4})$$

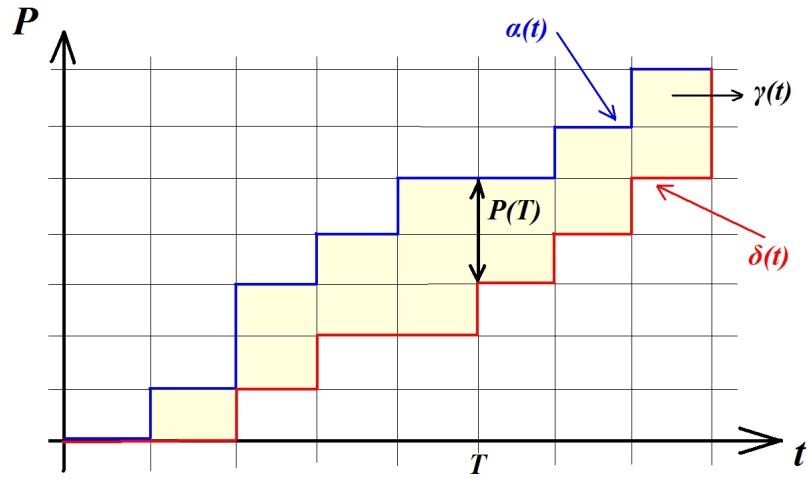


Figure A.1: Little's Theorem Representation

By using Equation A.2, A.3, and A.4 :

$$\gamma(t) = \bar{T}_t \alpha(t) \quad (\text{A.5})$$

$$\bar{P}_t = \frac{\bar{T}_t \alpha(t)}{t} = \lambda_t \bar{T}_t \quad (\text{A.6})$$

Now assume that the following limit exists:

$$\lim_{t \rightarrow \infty} \lambda_t = \lambda \quad (\text{A.7})$$

$$\lim_{t \rightarrow \infty} \bar{T}_t = \bar{T} \quad (\text{A.8})$$

Then,

$$\lim_{t \rightarrow \infty} \bar{P}_t = \bar{P} \quad (\text{A.9})$$

also exists and is given by  $\bar{P} = \lambda \bar{T}$ . ■